Algal Research 11 (2015) 134–147

Contents lists available at ScienceDirect

Algal Research

journal homepage: www.elsevier.com/locate/algal

Characterization of a *Chlamydomonas reinhardtii* mutant strain with improved biomass production under low light and mixotrophic conditions☆

Y. Zhou [a], L.C. Schideman [a,*], D.S. Park [b], A. Stirbet [c], Govindjee [d,e,f], S.I. Rupassara [g], J.D. Krehbiel [h], M.J. Seufferheld [i]

[a] Department of Agricultural and Biological Engineering, University of Illinois at Urbana Champaign, Urbana, IL 61801, USA
[b] Center for Biophysics and Quantitative Biology, University of Illinois at Urbana Champaign, Urbana, IL 61801, USA
[c] 204 Anne Burras Lane, Newport News, VA 23606, USA
[d] Department of Plant Biology, University of Illinois at Urbana Champaign, Urbana, IL 61801, USA
[e] Department of Biochemistry, University of Illinois at Urbana Champaign, Urbana, IL 61801, USA
[f] Center of Biophysics, and Quantitative Biology, University of Illinois at Urbana Champaign, Urbana, IL 61801, USA
[g] Institute for Genomic Biology, University of Illinois at Urbana Champaign, Urbana, IL 61801, USA
[h] Department of Mechanical Sciences and Engineering, University of Illinois at Urbana–Champaign, IL 61801, USA
[i] Department of Entomology—Illinois National History Survey, University of Illinois at Urbana–Champaign, Urbana, IL 61801, USA

ARTICLE INFO

Article history:
Received 24 June 2014
Received in revised form 6 May 2015
Accepted 4 June 2015
Available online xxxx

Keywords:
Chlamydomonas reinhardtii
Algal biofuels
Chlorophyll fluorescence transient
Metabolite profiling
Knock-out mutant
Non-photochemical quenching
Mixotrophic condition

ABSTRACT

Biophysical and biochemical characteristics of a spontaneous "mutant" strain (IM) of *Chlamydomonas reinhardtii* were quantified and compared with its progenitor (KO), a "knock-out" mutant with defects in phototaxis, and to its wild-type (WT); defects were shown to be preserved in the IM mutant. Growth curves showed that IM cultivated under mixotrophic conditions (TAP medium) and low light (10 and 20 μmol photons m^{-2} s^{-1}), had 5–27% higher dry cell weight than WT and KO. This advantage was most likely attributable to increased acetate metabolism because it was not observed under purely photoautotrophic conditions using high salt minimal medium. Further characterization of these strains grown under mixotrophic conditions revealed several other unique features for the KO and IM mutant strains. Specifically, the IM and KO cells, grown under 60 μmol photons m^{-2} s^{-1}, showed higher rates of net oxygen evolution and respiration than the WT cells. Further, the slow (minute range) SM rise phase of chlorophyll *a* fluorescence transient was much reduced in IM cells, which has been ascribed to a regulatory event, labeled as "*state 2 to state 1 transition*". Additionally, modulated fluorescence measurements showed that, when the IM strain is grown under low light, non-photochemical quenching of excited chlorophyll rises faster and recovers faster than in the other strains. Finally, compared to the WT, IM cells had a higher amount of metabolites related to carbon metabolism and protection against oxidative stress. These results suggest that the IM strain of *C. reinhardtii* has unique features that may be advantageous for improving algal biofuel production under mixotrophic conditions, such as algae cultivated in conjunction with wastewater treatment.

1. Introduction

Algae represent a promising new source of feedstock for the production of various renewable liquid biofuels [1,2] or hydrogen [3–5] with a low carbon footprint. Their diverse metabolic capability also makes algae a unique and versatile "crop" to produce various food ingredients, nutraceuticals, pharmaceuticals and animal feed [6]. Algae have several key advantages, including higher growth rates than terrestrial plants, the ability to grow on marginal lands and in low quality water sources, as well as the ability to take up excess nutrients from wastewater and eutrophic water sources [7], which provides important water quality benefits. Despite these significant advantages, the promise of algae for clean energy resources remains largely unfulfilled due to several practical bottlenecks in the production process. One important issue for the success of large-scale algal biomass production is maximizing biomass production under light limited conditions [8–10]. Due to rapid light attenuation in dense algal cultures, resulting from light absorption and scattering, significant spatial heterogeneity of light intensities occurs inside most photobioreactors. Cells at the lighted surface can be damaged

☆ This paper is dedicated to the memory of Robert M. Clegg (July 18, 1945–October 15, 2012), under whose direction David Park did the measurements shown in Fig. 5. Clegg was a pioneer of the "Physics of the Living Cells", and of Fluorescence Lifetime Imaging Microscopy (FLIM), and a very dear friend to all of us.

* Corresponding author.
E-mail address: schidema@illinois.edu (L.C. Schideman).

http://dx.doi.org/10.1016/j.algal.2015.06.001
2211-9264/

by excess light (through photoinhibition) [11] and lose absorbed radiant energy to heat dissipation. In contrast, cells located deeper in the culture may experience light limitations that would decrease cell growth. In addition, cultures grown in natural sunlight experience diurnal and seasonal fluctuations in lighting that have prolonged periods of low light intensity. Genetic and molecular studies have led to the development of strains that can tolerate high light and have better growth under high irradiance. For example, truncated antenna in algae can help improve light utilization efficiency by decreasing light absorption in the top layer cells, and enabling light to penetrate deeper into the cultures [12–17]. On the other hand, developing algal strains that increase biomass production under low light conditions is also advantageous because there are likely to be periods and places of low irradiance in large-scale algal production systems.

Another important issue for improving the feasibility of algal biofuels is to facilitate better integration with wastewater treatment. Cultivation of algae in wastewater has been considered as one of the most promising pathways to efficiently and economically produce algal biofuels [7,18]. Wastewater provides low-cost or, even free nutrient and water resources, as well as dual purpose infrastructure that can significantly reduce the net cost of algal biofuel production. For example, a recent comprehensive report by Lundquist et al. [19] showed that algal biofuels made with purchased inputs would exceed $400/barrel, but integration with wastewater inputs and infrastructure could lower the net costs of algal biofuel production to less than $30/barrel. To take better advantage of the potential synergies between wastewater treatment and algal biofuel production, algae strains are needed that have enhanced growth under mixotrophic conditions because wastewaters generally contain significant amounts of organic carbon. In addition, algal strains that grow well under low light conditions are also advantageous for cultivating algae in wastewater, which generally have higher turbidity and reduced light penetration.

We have chosen for our work a model green alga *Chlamydomonas reinhardtii* [20] in view of extensive prior knowledge and known advantages (see e.g., [21–23]). In particular, we note its advantage for biohydrogen production, when grown mixotrophically [24]. We present here our results from a variety of biophysical and biochemical characterization for three different strains of *C. reinhardtii*, a photoautotrophic green alga that can be also grown mixotrophically in acetate-supplemented media, such as Tris–acetate–phosphate (TAP). These algae remain green and retain normally developed chloroplasts under various growth conditions, due to their ability to use different reduced carbon sources, such as endogenous starch accumulated in the chloroplast during exposure to light, or exogenous organic carbon compounds like acetate, assimilated in the cytosol. This metabolic flexibility is due to a strong interaction between photosynthetic and non-photosynthetic carbon metabolisms (see Fig. 1). For information on their metabolism, see e.g., Boyle and Morgan [25] and Spijkerman [26], and for an extensive overview of the molecular biology of Chlamydomonas, see chapters in Rochaix et al. (eds.) [27].

A spontaneous "mutant" strain of *C. reinhardtii*, which we refer to as "IM" (for "immortal"), was discovered in our laboratory, which exhibits improved biomass production under low light intensity and mixotrophic conditions, which are advantageous features for algal biofuel production combined with wastewater treatment. The IM strain was obtained from a culture of the previously described knockout ptx2 mutant of *C. reinhardtii* (KO), which has defects in both phototaxis and photoshock responses related to impairment of light-induced flagellar currents [28]. The IM strain arose spontaneously after a long-term storage of KO cells, on a selective medium, in dim room light. In this study, we have investigated and compared the biophysical and biochemical characteristics of the IM strain, its progenitor, KO, and its wild type, WT, when grown under different light intensities, and under mixotrophic conditions, to better characterize the special features of the IM cells. By elucidating the distinctive characteristics of the IM and KO mutants, we provide useful insights on potential ways to improve practical algal biofuel production systems.

In order to better understand some of the measurements presented herein, such as chlorophyll fluorescence transient data, we provide a brief background on electron transfer pathways and carbon assimilation

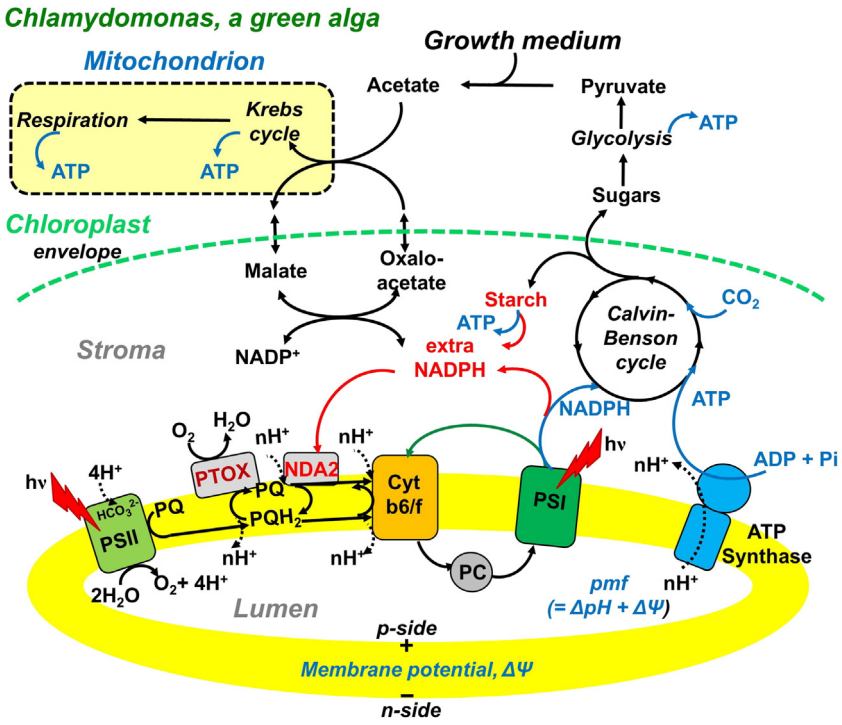

Fig. 1. Electron transfer pathways and carbon assimilation in the chloroplast of a mixotrophically (acetate) grown *Chlamydomonas reinhardtii*, and their interaction with mitochondrion. See text for further details.
Modified from Alric 2010 [29]. (For interpretation of the references to color in this figure, the reader is referred to the web version of this article.)

in the chloroplasts of Chlamydomonas cells, as shown in Fig. 1, which is adapted from Alric [29]. When a chloroplast is illuminated, the antenna of both photosystems, PSI and PSII, absorb light energy that is transferred rapidly to their reaction centers, P680 (PSII) and P700 (PSI), where primary charge separation (photochemistry) is initiated, followed by a chain of redox reactions. PSII ultimately oxidizes water and reduces electron carriers in the cytochrome (Cyt) b6/f, whereas PSI oxidizes Cyt b6/f, and reduces nicotinamide adenine dinucleotide phosphate (NADP+) to NADPH. In addition to the linear electron flow, ferredoxin-mediated cyclic electron flow also occurs around PSI (shown with a green arrow in Fig. 1). Further, a proton motive force, pmf (i.e., a pH gradient, ΔpH, plus a membrane potential, $\Delta\Psi$) is built across the thylakoid membrane during photosynthetic electron transfer, which is then used for ATP synthesis. The resulting NADPH and ATP are used in the Calvin–Benson cycle for CO_2 fixation that leads to the formation of sugars and starch. In mitochondria, acetate (both from the growth medium and that formed from glycolysis) is assimilated via acetyl-CoA into the Krebs (tricarboxylic acid) cycle. Extra NADPH and ATP can also be produced through starch breakdown in the chloroplast stroma; in addition, ATP may be produced through glycolysis in the cytosol [30]. Moreover, when respiration is inhibited, malate can accumulate in the mitochondrion, and be transferred to the chloroplast by a reversible malate/oxaloacetate shuttle, which generates extra NADPH. The excess reducing power can be transferred to the plastoquinone (PQ) pool via a monomeric type-II NADH in Chlamydomonas (i.e., NDA2, see [31]), and dissipated through the activity of plastid terminal oxidase (PTOX).

In summary, cooperation of two light reactions and two pigment systems leads to the production of reducing power (in the form of NADPH) and ATP, which are both subsequently used in the carbon-fixation pathway leading to the formation of carbohydrates. In Fig. 1, we also show that there is an interaction between chloroplasts and mitochondria, where acetate from the culture medium for growing Chlamydomonas may fit into the highlighted metabolic pathways.

2. Materials and methods

2.1. Algal strains and culture media

The wild type (WT) strain used was *C. reinhardtii* CC124. Pazour et al. [28] had previously constructed a knockout mutant (KO) of *C. reinhardtii* by insertional mutagenesis of the WT, which was totally deficient in light-induced flagellar currents. This KO strain is the progenitor of the spontaneous "immortal mutant" (IM) strain used in this study, which was discovered, in our laboratory, from a discarded KO culture that had a single surviving colony. "IM" appeared, in a sealed petri dish with selective agar medium, after a long period of storage under low and intermittent room light [32].[1]

All three strains of *C. reinhardtii* were maintained under room light (~30 μmol photons m^{-2} s^{-1}), at ~25 °C, and on tris–acetate–phosphate (TAP) agar culture medium plates (20 mM Tris(tris (hydroxymethyl)aminomethane); 17.4 mM acetate; 7 mM NH_4Cl; 0.4 mM $MgSO_4$; 0.3 mM $CaCl_2$; 1 mM phosphate buffer; 1 ml/l Hutner's trace metal solution; 15 g/l Bacto agar). Prior to each experiment, algal colonies from the agar plates were used to inoculate stock cultures made in 250 ml Erlenmeyer flasks with 50 ml of liquid TAP medium (without Bacto agar) that were mixed on an orbital shaker at 24 °C under 20 μmol photons m^{-2} s^{-1} of photosynthetically active radiation (PAR) provided by fluorescent lamps. High salt minimal medium (HSM), of the same composition as the TAP medium, but without acetate (where the final pH = 7 was adjusted using HCl), was also used for the measurement of growth curves. However, unless specifically noted otherwise, all the other experiments presented below were done with algae suspended in TAP medium.

2.2. Phototaxis assays

For phototaxis experiments, all three Chlamydomonas strains were grown using 50 ml of TAP medium in 125 ml Erlenmeyer flasks for seven days with continuous fluorescent lighting at 760 lm. The number of cells were counted, and then diluted to a concentration of 4×10^6 cells/ml in small glass tubes holding 5 ml aliquots. Four replicates of each strain were dark-adapted for at least 1 h prior to testing for phototaxis. The procedure used to determine phototaxis properties of the algae was similar to that reported previously by Pazour et al. [28]. Initially, each sample was shaken 8 times in the tubes, to ensure a uniform initial distribution of the cells. Then, the tubes were placed 60 cm away from a 250 W halogen bulb (intensity of 305 lm) and irradiated for 3 min. When phototaxis is normal, a clear band is supposed to form at the back of the tube, as the cells swim to the backside of the tube and form a tight vertical band on the glass. Cells that do not exhibit this phototaxic response can be readily identified as having phototaxis defects. This process was repeated with samples situated also at 30 cm from the light source (intensity: 1430 lm).

2.3. Algal growth curves under different light intensities

2.3.1. Mixotrophic cultivation

WT, KO and IM cells were grown in TAP medium at three different light intensities: 10 ± 1, 20 ± 2 and 640 ± 5 μmol photons m^{-2} s^{-1}, where the average and standard deviation of these light intensities were determined by measurements at least at 9 positions covering the locations of various culture flasks on the shaker table. For the lowest light intensity experiments, light was produced by two 25 W fluorescent lamps. Four 25 W fluorescent lamps were placed on top of a shaker table to produce 20 μmol photons m^{-2} s^{-1}. For the highest light intensity, six 42 W compact fluorescent bulbs were placed directly over each culture flask. Culture flask positions were also rotated regularly to minimize any differences in light intensity. For growth experiments, cultivation of each algal strain was initiated in duplicate with a starting cell density of 10,000 cells/ml. Cell growth was measured as dry cell weight, and duplicate measurements of samples from each culture flask were averaged to determine the growth curves for each strain and each lighting condition. Dry cell weight was measured as total suspended solids according to standard methods [33].

2.3.2. Photoautotrophic cultivation

As mentioned earlier, a photoautotrophic growth experiment in HSM medium was also conducted for all three algae strains grown under the low light condition of 10 μmol photons m^{-2} s^{-1} and under identical conditions as used in mixotrophic cultivation described above. Algal cell density was measured both as optical density (OD) at 750 nm (using a Tecan® 200 PRO reader (Männedorf, Switzerland)) and as dry cell weight. Cultivation of each algal strain was initiated in duplicate with a starting OD at 750 nm of 0.1.

2.4. Photosynthetic oxygen evolution measurements

Rates of oxygen evolution, for WT, KO and IM cells, were measured using a Clark-type oxygen electrode (Hansatech Instruments Limited). Algae were cultivated in TAP medium under light intensity of 60 μmol photon m^{-2} s^{-1}. Cells in the exponential growth phase (48 h after inoculation) were used for these tests. Chlorophyll (Chl) concentration of samples was adjusted to 15 μg/ml, and then the samples were suspended in 20 mM HEPES buffer (pH 7.4) before oxygen evolution measurements. Rates of oxygen evolution were measured as a function of increasing light intensity using red LED light (peak intensity at 650 nm): 0, 20, 200, 400, 600 and 800 μmol photons m^{-2} s^{-1},

[1] A preliminary report on the "IM" mutant was first presented by Zhou et al. [32] at the 15th International Conference on Photosynthesis in Beijing, China.

with each light intensity being maintained for 2 min during oxygen measurements. Three separate cultures of each strain were used for this experiment, and duplicate measurements were made for each culture replicate; thus, oxygen evolution data are presented as the average of six measurements (n = 6). Oxygen evolution rates were then normalized based on Chl concentrations, and are reported as μmol O_2 mg Chl^{-1} h^{-1}.

2.5. Chlorophyll a fluorescence transient measurements

Chl *a* fluorescence transients were measured at room temperature (~21 °C) with a Handy PEA (Plant Efficiency Analyzer, Hansatech Instruments Ltd.) by using a saturating excitation light (λ 650 nm) of 3000 μmol photons m^{-2} s^{-1} for 300 s. A Corning RG9 cut-off filter was placed before the photodetector to avoid measuring the excitation light (650 nm), and to measure Chl fluorescence beyond 690 nm. The algal cultures used in these experiments were grown in TAP medium at either 20 μmol photons m^{-2} s^{-1} (low light) or 640 μmol photons m^{-2} s^{-1} (high light), and samples were taken from the exponential growth phase (48 h after inoculation). Before fluorescence measurements, cell suspensions were placed in flasks, with stirring, under room illumination (~30 μmol photons m^{-2} s^{-1}). Three separate culture replicates of each strain were used for these experiments, and triplicate measurements were made for each culture replicate (n = 9). All algal samples were adjusted to have a Chl concentration of 15 μg/ml before measurements. These samples, suspended in TAP medium, were dark adapted for 6 min prior to measurement of the fast (up to 1 s) fluorescence transients (labeled as OJIP transients, see below), which were analyzed according to methods described in earlier publications [34–37]. A number of fluorescence parameters were evaluated based on fluorescence values measured at specific times on the OJIP curves, where O (origin) is the initial minimum fluorescence, which is followed by a rise to inflection points J and I, and then finally to the peak P [38]. Six fluorescence values were used in this analysis: F_o, at 0.02 ms; F(0.1), at 0.1 ms; F(0.3), at 0.3 ms; FJ, at 2 ms; FI, at 30 ms; and F_m (the maximum fluorescence), at the P level [34]. (For an example of using Chl fluorescence in biomass research, see e.g., Toepel et al. [39])

2.6. Measurement of non-photochemical quenching (NPQ) of the excited state of chlorophyll

A Pulse Amplitude Modulation (PAM) portable fluorometer (PAM-2100, Heinz Walz GmbH), in saturating pulse (SP)-mode, was used for the evaluation of chlorophyll fluorescence parameters associated with the slow (up to minutes) fluorescence induction. Chl *a* fluorescence was measured at room temperature (~21 °C), with a weak modulated measuring light (~0.1 μmol photons m^{-2} s^{-1}; λ = 650 nm, modulated at 0.6 kHz). As noted above, Chl concentration in each sample was 15 μg/ml before measurement. Cells of all three strains, IM, KO and WT (each suspended in TAP medium) were placed in a chamber designed for PAM fluorescence measurements of liquid cultures, with automatic stirring to prevent settling.

The following protocol was used for PAM measurements: (1) Chlamydomonas cells were first dark adapted for 5 min; (2) the minimum level of fluorescence, F_o, was then measured, after which a saturating light pulse (8000 μmol photons m^{-2} s^{-1}; λ = 665 nm, modulation frequency of 20 kHz) was applied, leading to an increase of fluorescence yield up to its maximum value (F_m); (3) after ~40 s of darkness, an actinic light (~600 μmol photons m^{-2} s^{-1}; λ = 665 nm) was turned on for 5 min, during which repeated pulses of saturating light (at ~20 s intervals) were applied; at each light pulse, the fluorescence increased to a value $F_{m'}$ (maximum fluorescence in light); and (4) the actinic light was turned off, and another train of saturating light pulses at ~20 s or longer intervals was applied for 15 min.

Non-photochemical quenching (NPQ) of the excited state of chlorophyll was calculated according to the following equation [40]: NPQ = (F_m − $F_{m'}$) / $F_{m'}$, where, Fm′ is the maximum fluorescence in light, and F_m is the maximum fluorescence in the dark-adapted sample. Three independent cultures of WT, KO and IM cells were used for these experiments, and triplicate measurements were made for each independent culture (n = 9). For a detailed discussion on all aspects of NPQ, see chapters in Barbara Demmig-Adams et al. (Eds.) [41].

2.7. Metabolite profile analysis

Metabolite profiling of the IM and WT algal strains during exponential growth phase was conducted according to methods described earlier [42–44]. Algal cells, collected during the exponential growth phase under low light (20 μmol photons m^{-2} s^{-1}) and high light (640 μmol photons m^{-2} s^{-1}), were first lyophilized, and then metabolites were extracted from 25 mg of dried and homogenized cells, using 0.7 ml of ~100% methanol. The extraction mixtures were shaken on a VSM-3 shaker (Pro Lab Plus Series, Pro Scientific Inc.) for 5 min, incubated at 67 °C for 5 min, vortex mixed and then centrifuged at 13,000 rpm for 3 min. Supernatants were collected and kept at −20 °C, and the pellets were extracted a second time following the same procedure, except that the solvent used was 70% methanol (adjusted to ~pH = 6.0 with 0.1 M HCl) and the extraction mixture was incubated at 45 °C for 5 min. Supernatants, obtained after a second extraction, were added to the first extracts and stored at −20 °C. The pellets were extracted in the same manner a third time using 0.6 ml chloroform and incubation at 45 °C, and these extracts were added to the previous extracts, and then the combined extracts were vacuum-dried, using a Savant SpeedVac. The dried extracts were stored at −20 °C until derivatization was performed. These dried extracts were then added to an internal standard (10 mg ml^{-1} of hentriacontanoic acid in 10 μl of pyridine), and vacuum dried. The metabolites were then derivatized using methoxyamine hydrochloride, followed by trimethylsilylation with N-methyl-N-(trimethylsilyl) trifluoroacetamide (final volume, 150 μl) and analyzed by gas chromatography–mass spectrometry (GC–MS), as described previously [44]. ChemStation and Amdis software were used for data acquisition and deconvolution of the chromatographic peaks. Subsequently, extracted metabolites were identified by comparing their mass spectra with those available in several mass spectral libraries (NIST05, Golm Metabolome Database; http://gmd.mpimp-golm.mpg.de/; and personal libraries). Information on the amount of metabolites in different samples was based on their relative abundance compared with the internal standards. Since all samples were prepared using the same amount of biomass, extraction solvents and internal standard, the results are normalized based on dry cell weight and can be directly compared.

3. Results

3.1. Phototaxis behavior

All the tubes containing the WT strain clearly showed the dark line indicative of negative phototaxis (i.e., swimming away from the light; see Section 2.3.2). None of the KO or IM samples showed such a line (see Supplementary material Fig. S1, for representative pictures of results on phototaxis behavior). Thus, our experiments show that the phototaxis defects of the KO progenitor, resulting from “knock out” genetic manipulation, are indeed conserved in the spontaneous IM mutant.

3.2. Cell growth under different light conditions

Fig. 2 shows growth curves for each of the three Chlamydomonas strains used in this study in terms of dry cell weight. This figure includes data for mixotrophic growth in TAP media under two low light

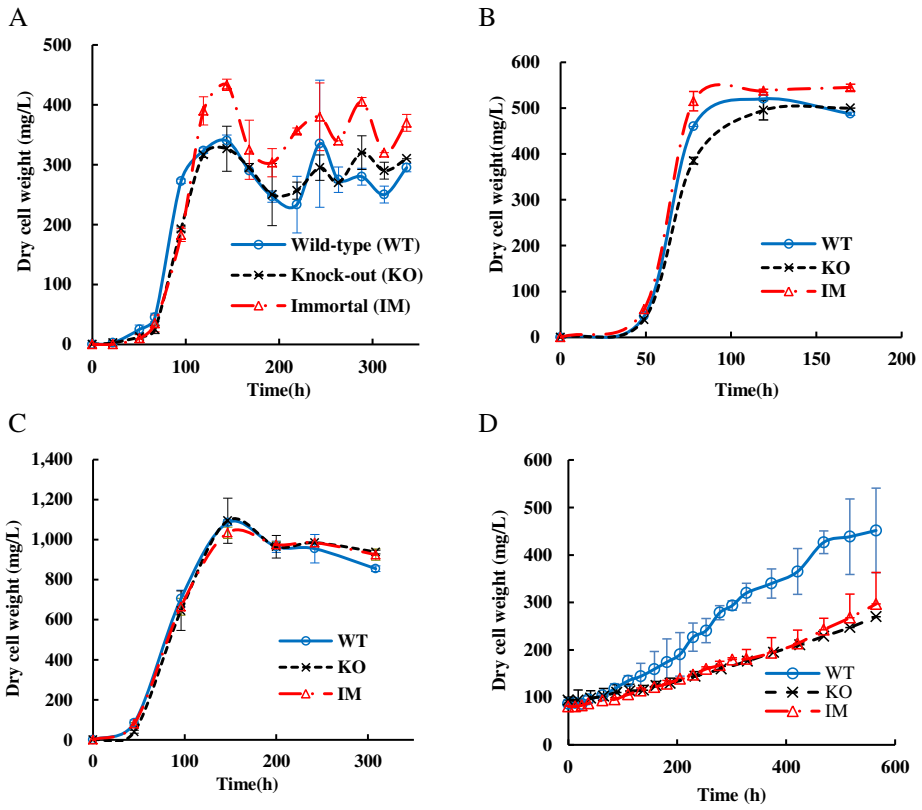

Fig. 2. Dry cell weight growth curves of *Chlamydomonas reinhardtii* algae grown at 24 °C under fluorescent light of three different light intensities for three different strains: wild-type (WT), knock-out mutant (KO) and spontaneous mutant (IM). (A) 10 μmol photons m^{-2} s^{-1}; TAP medium; (B) 20 μmol photons m^{-2} s^{-1}; TAP medium; (C) 640 μmol photons m^{-2} s^{-1}; 1; TAP medium; (D) 10 μmol photons m^{-2} s^{-1}; HSM medium. Two culture replicates were used, and average values are plotted with error bars showing the standard deviation.

intensities (10 and 20 μmol photons m^{-2} s^{-1}) and one high (saturating) light intensity (640 μmol photons m^{-2} s^{-1}). In addition, Fig. 2 presents a photoautotrophic growth curve for one low light intensity (10 μmol photons m^{-2} s^{-1}).

Under mixotrophic conditions, with a light intensity of 10 μmol photons m^{-2} s^{-1}, all three Chlamydomonas strains reached their maximum dry cell weight at 144 h of growth. At this time, the IM strain had maximum dry cell weight of 433 mg/l, which was 27% higher than that of the WT cells; however, KO and WT cells had an almost identical maximum dry cell weight (Fig. 2A). At a light intensity of 20 μmol photons m^{-2} s^{-1} (Fig. 2B), the IM strain still showed slightly higher maximum biomass production compared to other strains, but the advantage was reduced. Specifically, the IM cells had a maximum dry cell weight of 545 mg/l after 170 h of growth, which was 5% higher than the maximum dry cell weight of WT cells (520 mg/l after 119 h). This difference was statistically significant (p value of 0.0377 in two tailed *t*-test). Finally, under our high light condition (640 μmol photons m^{-2} s^{-1}), all the samples (the IM, KO and WT cells) showed very similar (no statistically significant difference) maximum biomass production after 147 h, as shown in Fig. 2C.

In order to determine if the advantage in biomass production under low light conditions for the IM strain was primarily related to the presence of acetate in the growth medium or to their photosynthetic capacity, a photoautotrophic growth experiment with cells suspended in HSM medium was also conducted under the low light intensity of 10 μmol photons m^{-2} s^{-1}, the condition in which the IM strain showed its biggest relative advantage for biomass production. As shown in Fig. 2D, under purely photoautotrophic conditions, the WT cells actually had the highest maximum biomass dry cell weight of 451 mg/l after 565 h, which was 67% higher than that measured in KO (270 mg/l), and 52% higher than that in IM cells (297 mg/l). This result suggests that the advantage of the IM strain, under low-light mixotrophic conditions, is probably primarily related to improved acetate metabolism.

3.3. Oxygen evolution

Fig. 3 shows net photosynthetic O_2 evolution rates (Pn) as a function of light intensity (Pn–E curves) for WT, KO and IM cells of *C. reinhardtii* grown mixotrophically under 60 μmol photons m^{-2} s^{-1}. The KO and IM cells showed significantly higher net O_2 evolution rates than the WT cells (see Table 1). The highest light intensity used in our experiment (800 μmol photons m^{-2} s^{-1}) resulted in maximum net O_2 evolution

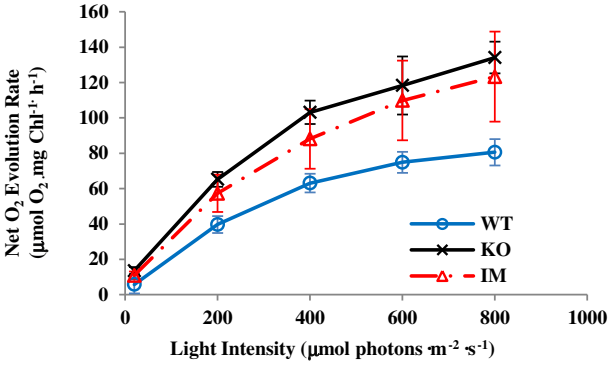

Fig. 3. Net photosynthetic O_2 evolution rate (P_n) as a function of light intensity (P_n–E curves) for WT, KO and IM cells of *Chlamydomonas reinhardtii* cultured in TAP medium under fluorescent light of 60 μmol photons m^{-2} s^{-1}, and collected during the exponential growth phase. The light source was a red LED with a peak wavelength at 650 nm. Three separate culture replicates were used and duplicate measurements were made for each culture replicate (n = 6); results are presented as averages ± standard deviations.

Table 1
Rates of photosynthesis and respiration, calculated from the P_n–E curves, of all three Chlamydomonas strains (average values ± standard deviations for six replicate measurements) grown in TAP medium under 60 μmol photons m^{-2} s^{-1} light intensity.

	WT	KO	IM
P_{max}, maximum net O_2 evolution rate (μmol O_2 mg^{-1} Chl *a* h^{-1})	80.6 ± 7.5	134.1 ± 8.9	123.3 ± 25.4
R_d, dark respiration rate (μmol O_2 mg^{-1} Chl *a* h^{-1})	25.0 ± 3.4	40.3 ± 8.7	35.2 ± 5.3

rates per chlorophyll (P_{max}), which were approximately 1.5 times higher in KO and IM cells than in WT cells.

Further, our measurements showed that KO and IM cells have 1.6 and 1.4 times higher dark respiration rates than the WT cells (Table 1). As a general rule, the greater the metabolic activity of a photosynthetic organ or tissue, the higher its respiration rate [45]. Therefore, the KO and IM cells are very likely to have more active metabolism than the WT cells.

3.4. Chlorophyll a fluorescence transient

3.4.1. The fast (up to a second) chlorophyll a fluorescence transient

Chl *a* fluorescence induction data is a rapid, noninvasive, sensitive, and accurate method that continues to be used in a large number of photosynthesis studies [38,46–49]. Here we measured Chl *a* fluorescence transients for each of the strains grown under mixotrophic conditions with saturating 650 nm light (3000 μmol photons m^{-2} s^{-1}), which allowed us to characterize PSII activity. Our results for KO and IM cells show some similarities, but also some differences, in comparison to those for WT cells, grown under both low and high light conditions, as discussed below.

The fast (up to 1 s) Chl *a* fluorescence transients, as shown in Fig. 4A and B, were normalized both at O (F_o) and P (F_m) levels to obtain the relative variable fluorescence, $V(t) = (F(t) - F_o)/(F_m - F_o)$; this double normalization allows us to compare fluorescence transients measured in different samples [35]. (The original data before normalization are provided in Fig. S2 of the Supplementary data for this paper.) Fig. 4A shows that, when grown under low light (20 μmol photons m^{-2} s^{-1}), the fast fluorescence induction curves of all three Chlamydomonas strains (i.e., WT, KO and IM) show three characteristic phases, O–J, J–I, and I–P [50]. These OJIP curves have quite similar shapes in all three samples, with only a slightly steeper J–I rise and a slightly higher I level (~5–10%) in the curves for IM cells. In order to highlight these differences, relative variable fluorescence of the WT cells was subtracted from that of the IM and KO cells [51] and shown in Fig. 4C. Indeed, the curve (IM–WT) shows a clear difference in the I-band.

For samples grown under high light (640 μmol photons m^{-2} s^{-1}), the J step in all Chl *a* fluorescence curves is no longer discernible, while the I and P steps are still clearly seen (see Fig. 4B). Differences between the fluorescence transients of Chlamydomonas strains grown under high light (see Fig. 4D) were more noticeable than between those grown under low light, both before and after normalization (see Supplementary Fig. S2B for data before normalization). In particular, the fluorescence transients measured in KO cells showed a less steep O–I fluorescence rise and a lower I level (~15–20%) than in WT and

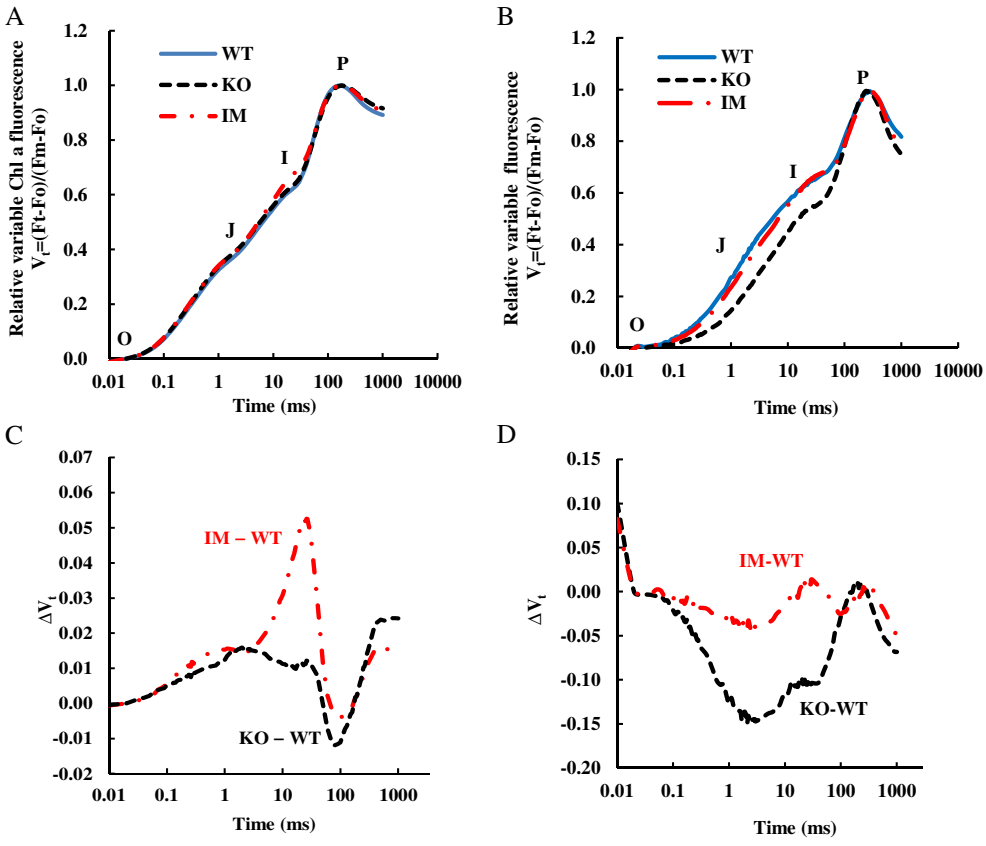

Fig. 4. The fast chlorophyll *a* fluorescence transient, up to 1 s, in WT, KO, and IM *Chlamydomonas reinhardtii* strains grown in TAP medium under fluorescent light of (A) 20 μmol photons m^{-2} s^{-1} (low light) or (B) 640 μmol photons m^{-2} s^{-1} (high light). Data were double normalized at F_o and F_m, and are presented on a logarithmic time scale in the 0–1 s range; data points are averages of nine independent measurements. (C) and (D) Difference curves (IM–WT) and (KO–WT) of the respective fluorescence transients shown in panels (A) and (B). The symbol O (the origin) refers to the minimum fluorescence, P (peak) to the maximum fluorescence, and J and I are inflections between the two.

IM cells. The reduced O–I fluorescence rise for KO cells probably reflects a smaller PSII antenna size [35]. The lower I level for KO is likely related to a faster electron flow from Q_A^- to PSI acceptors due to an increased PSI/PSII ratio or a larger PSI antenna size [35,52,53].

Although many fluorescence parameters have been defined for the analysis of the OJIP transient in the literature [36,48,54], we present here only a few of the key fluorescence parameters commonly used for the characterization of photosynthetic samples (see Table 2).

3.4.1.1. Minimum (F_o), maximum (F_m), and variable (F_v) fluorescence. Both the initial fluorescence (F_o) and maximum fluorescence (F_m) had relatively close values in the IM and KO strains grown under low light (20 μmol photons m^{-2} s^{-1}), and the differences between the WT cells and the two mutants were less than 12.5% for F_o, and less than 16% for F_m (see Table 2). Therefore, the F_v/F_m ratios (where $F_v = (F_m - F_o)$ is the maximum variable fluorescence) were also very similar (i.e., ~0.78) for all Chlamydomonas strains grown under low light and mixotrophic conditions. The F_v/F_m ratio is widely used in photosynthetic studies as a proxy for the maximum efficiency of PSII photochemistry [55]; the rationale for this has been described, e.g., by Govindjee [56]. A higher F_v/F_m value (i.e., >0.76) is generally correlated with higher photosynthetic performance [38], but only in the presence of similar CO_2 levels, and in the absence of alternative electron sinks. Even though we found that IM and KO cells had a slightly higher maximum efficiency of PSII photochemistry compared to WT cells (i.e., +1.2% and +1.9%, respectively), the difference between WT and KO cells for this parameter was not statistically significant according to the *t*-test, which had a p value of 0.2751. However, the difference between the WT and the IM was statistically significant with a p value of 0.0022.

In contrast, F_o and F_m measured in samples grown under high light showed much greater differences between the strains (see Table 2). The KO strain had a very low F_o, which was the lowest among the three strains, while the other two had higher F_o values. The F_o value in the KO strain grown under high light was also lower (−24%) than those measured in low light grown cells, while the F_o values of WT and IM strains grown under high light were higher than those in low light grown cells (i.e., +74% and +37% for WT and IM strains, respectively). However, the slopes of the initial O–J fluorescence rise (see dV/dto values in Table 2) in WT and IM cells were higher than in the KO cells. Further, the increased apparent F_o value, observed in our data, is probably the result of a partial reduction of Q_A even after the dark adaptation period, due to a partially reduced PQ-pool [57]. We note that the F_m values were much lower in cells grown in high light than for cells grown under low light (see Table 2), especially in the KO strain, which had the lowest F_o and F_m values. (For possible explanations, see discussion elsewhere [35,58].) In all Chlamydomonas cells grown under high light, the maximum quantum yield of PSII photochemistry had lower values (less than 0.62; see Table 2). Our data are in agreement with results obtained in other studies with Chlamydomonas grown at different light intensities, which also showed a reduction of F_v/F_m in high light compared to that in low light [59]. The low F_v/F_m values measured in WT and IM cells (i.e., 0.4 and 0.57, respectively) may be partially due to a high apparent F_o value, as mentioned above.

3.4.1.2. The ratios of F_v to F_o, and of F_o to F_m. The ratio F_v/F_o, a parameter also used as an indicator of potential PSII photochemistry and CO_2 fixation capacity, was also higher in KO (+6.7%) and IM (+8.9%) cells than in WT cells for samples grown under low light and mixotrophic conditions.

Another important parameter is the ratio F_o/F_m, which is a measure of the efficiency of energy de-excitation in PSII, as $F_o/F_m = k_N / (k_N + k_P)$, where k_N is the global rate constant of all non-photochemical de-excitation processes for Chl *a* in PSII antenna (which includes fluorescence, heat and energy transfer to another PSII or PSI); and kP is the rate constant for photochemical de-excitation at the PSII reaction center level [35]. This parameter had fairly similar values in all samples grown under low light, but was slightly higher in the IM and KO cells (see Table 2). For cells grown under high light, F_o/F_m ratios were significantly higher than in the same cells cultured under low light; however, in WT and IM cells these values are probably overestimated due to a higher apparent F_o, as mentioned above.

3.4.2. The slow phase of chlorophyll a fluorescence transient (from 1 s to 300 s)

After the OJIP phase, Chl *a* fluorescence declines to a semi-steady state, the "S" level, and this is followed by a rise to an M (maximum) level, which is followed by a decline to a terminal steady state level, T [60,61]. Fig. 5 shows our fluorescence data for the three Chlamydomonas strains in TAP medium (grown under low light) during the SMT phase, which is in the range of minutes. We note that the

Table 2
Comparison of selected chlorophyll *a* fluorescence parameters (see text for details) of the WT, KO and IM strains of *Chlamydomonas reinhardtii* for cultures grown in TAP medium under fluorescent lamps of two different light intensities (20 and 640 μmol photons m^{-2} s^{-1}) and sampled during the exponential phase. Shown are averages ± standard deviations for at least nine replicate measurements.

Fluorescence parameter symbols	Fluorescence parameter description	Wild-type (WT)	Knock-out mutant (KO)	Immortal mutant (IM)	(KO-WT)/WT	(IM-WT)/WT
Low light condition: 20 μmol photons m^{-2} s^{-1}						
F_o	Initial (minimum) Chl fluorescence intensity	217 ± 34	244 ± 19	235 ± 9	12.5%	8.3%
F_m	Maximum Chl fluorescence intensity	954 ± 185	1115 ± 75	1097 ± 69	16.0%	15.0%
F_v/F_m	Reflects maximum quantum yield of PSII photochemistry	0.77 ± 0.01	0.78 ± 0.02	0.79 ± 0.01	1.2%	1.9%
F_v/F_o	The ratio of maximum variable ($F_v = F_m - F_o$) Chl fluorescence and initial fluorescence	3.37 ± 0.2	3.60 ± 0.49	3.67 ± 0.24	6.7%	8.8%
F_o/F_m	Reflects quantum yield of excitation energy dissipation	0.23 ± 0.01	0.22 ± 0.02	0.21 ± 0.01	−4.0%	−6.3%
dV/dto	The initial slope of the double normalized (to F_o and F_m) Chl fluorescence transient	0.684 ± 0.01	0.71 ± 0.08	0.73 ± 0.02	4.5%	6.2%
High light condition: 640 μmol photons m^{-2} s^{-1}						
F_o	Initial (minimum) Chl fluorescence intensity	377 ± 58	185 ± 6	322 ± 10	−50.9%	14.5%
F_m	Maximum Chl fluorescence intensity	626 ± 35	490 ± 37	754 ± 85	−21.7%	20.4%
F_v/F_m	Reflects maximum quantum yield of PSII photochemistry	0.40 ± 0.08	0.62 ± 0.04	0.57 ± 0.05	55.1%	41.8%
F_v/F_o	The ratio of maximum variable ($F_v = F_m - F_o$) Chl fluorescence and initial fluorescence	0.69 ± 0.23	1.66 ± 0.26	1.34 ± 0.25	139.3%	93.4%
F_o/F_m	Reflects quantum yield of excitation energy dissipation	0.60 ± 0.08	0.38 ± 0.04	0.43 ± 0.05	−36.8%	27.9%
dV/dto	The initial slope of the double normalized (to F_o and F_m) Chl fluorescence transient	0.41 ± 0.09	0.19 ± 0.02	0.34 ± 0.03	−54.7%	16.3%

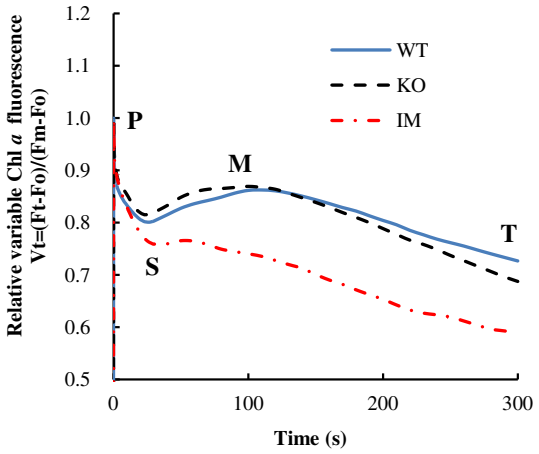

Fig. 5. The slow chlorophyll *a* fluorescence transient, up to 5 min, of three *Chlamydomonas reinhardtii* strains (WT, KO, and IM) grown in TAP medium under 20 μmol photons m^{-2} s^{-1} fluorescent light. Data were double normalized at F_o (O level) and at F_m (P level) and are presented as the average values of at least nine independent measurements. The symbol S refers to semi-steady state level, M to another maximum (appearing at longer time than P) and T refers to a terminal steady state.

IM strain did not show a S–M fluorescence rise, in contrast to the KO and WT strains; this suggests that the IM strain may have a reduced capacity to go from a low fluorescence state (State 2) to a high fluorescence state (State 1) (see Discussion section); this speculation for the SM rise is based on the observations of Kaňa et al. [62] on the absence of this rise in a *Synechocystis* mutant (Rpa C−) that is locked in State 1, and those of Kodru et al. [63] on drastically reduced S–M rise in the stt7 mutant of *C. reinhardtii*, which is also locked in State 1 [64]. Further research is needed to fully understand the implications of this observation.

3.5. Non-photochemical quenching analysis

The non-photochemical quenching (NPQ) of the excited state of Chl *a* is a process that down-regulates excitation pressure in the photosynthetic apparatus by increasing de-excitation, as heat, of the singlet excited state of Chl *a* (see Demmig-Adams et al. [41,65]), in parallel with a decrease in Chl *a* fluorescence yield. We present and discuss here results on the kinetics of NPQ induction and its relaxation, as obtained by using a PAM instrument (Walz) for the three different Chlamydomonas strains grown and tested under mixotrophic conditions (TAP medium), using both low light (20 μmol photons m^{-2} s^{-1}; Fig. 6A) and high light (640 μmol photons m^{-2} s^{-1}; Fig. 6B). Our data show that the maximum fluorescence values (F_m, F_m') in samples grown under low light were significantly higher than those grown under high light. This agrees with the fluorescence results presented in Table 2, obtained with a HandyPea instrument (Hansatech).

As shown in Fig. 6C, WT cells, grown under low light conditions, had biphasic NPQ induction kinetics, with the first phase characterized by a fast NPQ increase that reached a maximum, and then slightly decreased to a plateau in the second phase after approximately 100 s of

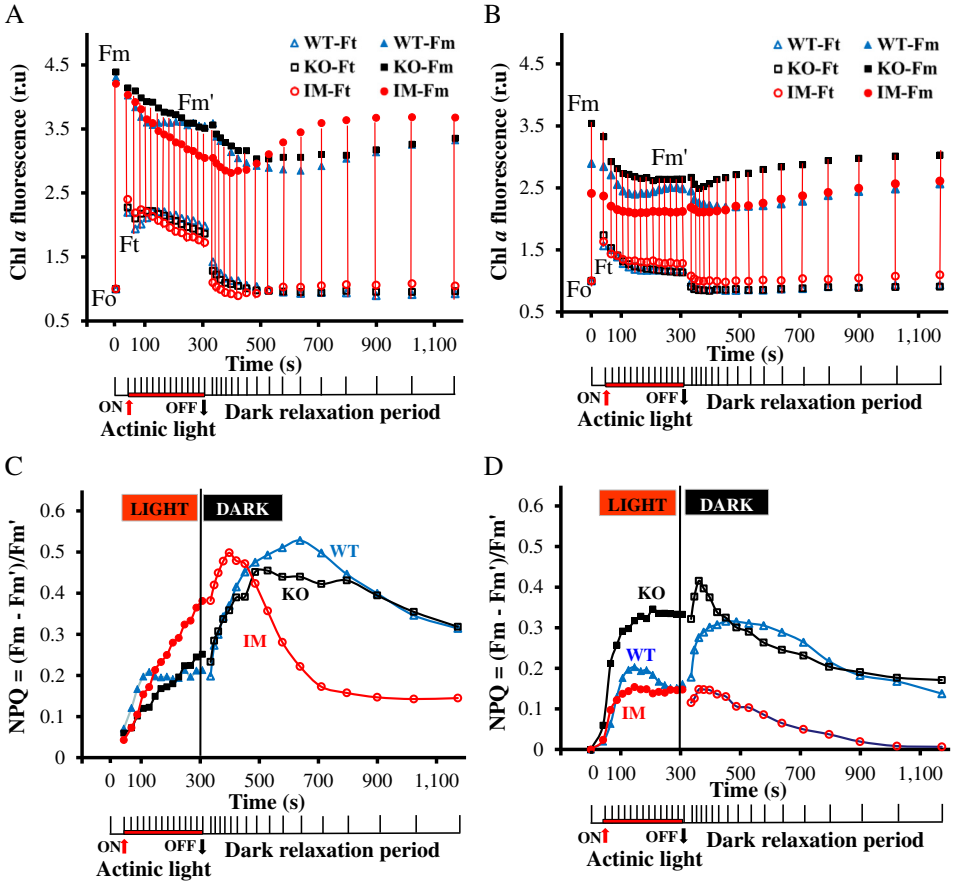

Fig. 6. Chlorophyll *a* fluorescence data obtained with Pulse Amplitude Modulation (PAM) instrument (Walz) in saturated pulse mode for three Chlamydomonas strains (WT, KO and IM) grown in TAP medium under fluorescent lamps of (A) low light (20 μmol photons m^{-2} s^{-1}) and (B) high light (640 μmol photons m^{-2} s^{-1}); (C) Nonphotochemical quenching (NPQ) kinetic curves obtained using the data shown in (A); and (D), NPQ kinetic curves obtained using the data shown in (B). Data points are averages of nine independent measurements and normalized at the "O" level (F_o). During the 5 min "Light" period, samples were illuminated with 665 nm actinic light (~600 μmol photons m^{-2} s^{-1}) and 665 nm saturating pulses (8000 μmol photons m^{-2} s^{-1}) every 20 s, or longer (time sequence of these light pulses is shown in the lower part of each panel). The actinic light was turned off during the 20 min "Dark" relaxation period, but the samples still received the series of saturating light pulses.

illumination with actinic light. On the other hand, IM and KO mutant cells had NPQ that increased steadily through the actinic illumination period, but at a slower rate initially than in the WT cells. At the end of the illumination period, NPQ in the IM cells had a significantly higher value than in both the WT and KO cells. After the actinic light was turned off, the NPQ continued to increase in all samples (but to a much lesser extent in the IM cells), and reached maximum values at 80 s, 200 s and 400 s for IM, KO and WT cells, respectively (see Fig. 6C). The WT cells reached the highest NPQ value, but it was close to the maximum NPQ level for the IM cells. During the NPQ relaxation process that followed, the most dramatic difference between these samples was that NPQ in the IM cells decreased much faster, and reached a much lower value than in the KO and WT cells. For all three strains, the fluorescence recovery was still not complete at the end of the measurement, indicating that the cells were somewhat photoinhibited, and/or some other NPQ process characterized by slow dark recovery was present [66], but the IM cells had significantly better dark NPQ recovery than the WT and KO strains.

The NPQ kinetics for Chlamydomonas cells grown under high light (Fig. 6D) showed similar biphasic NPQ induction patterns in all the three strains, with a rapid NPQ increase, followed by a plateau, but the KO strain reached a higher NPQ value than the IM and WT strains. We note, however, that the NPQ in the WT strain decreased transiently after 100 s actinic illumination. After the actinic light was turned off, the NPQ in WT and KO continued to increase for 50 s and 150 s, respectively (see Fig. 6D), but it did not increase in IM cells. After reaching the peak, NPQ gradually relaxed in all three strains, but only in IM cells, it recovered completely during the dark (relaxation) period.

3.6. Metabolite profiling

Since differences in cellular activity other than photosynthesis were suspected of being affected in IM cells, we performed metabolite profiling analysis to obtain insight into the complex regulatory processes and to better understand the reasons behind the higher biomass production in the IM cells grown under low light. The metabolite profiling revealed some potentially advantageous differences in IM cells over WT cells grown mixotrophically in TAP medium under both low and high light conditions. Fig. 7 shows a comparison of the relative quantities of some selected metabolites produced in WT and IM cells during the exponential growth phase under both low light (20 μmol photons m^{-2} s^{-1}) and high light (640 μmol photons m^{-2} s^{-1}) (see Table S1 in the Supplementary data for a more complete list of metabolic compounds measured).

First, the IM cells grown under low light showed increased quantities of several important metabolites related to carbon metabolism. For instance, under 20 μmol photons m^{-2} s^{-1}, IM cells had higher amounts of key sugars including ribose, fructose, maltotriose and glucose than WT cells (1.3–11.5 fold higher). In addition, IM had more sugar phosphates such as fructose-6-phosphate and mannose-phosphate (2.4 and 7.2 fold higher than WT, data not shown). However, under high light (640 μmol photons m^{-2} s^{-1}), these sugars and sugar phosphates were at much lower levels in the IM cells (0.2–1.2 fold) compared to the WT cells, as shown in Fig. 7A.

Under low light, IM cells also had much higher levels of key organic acids than the WT cells, such as glyceric acid, gluconic acid and malic acid (3–24 fold higher); however, under high light, these metabolites were at much lower levels (0.3–0.9 fold) compared with the WT cells, as shown in Fig. 7A. Since these sugars and organic acids are either photosynthetic products or intermediates during carbon metabolism [67] that are closely related to energy production in photosynthesis, we suggest that the high level of these key sugars and acids in IM cells under low light conditions could be related to the advantageous biomass production of IM cells observed under low light conditions, and grown under mixotrophic conditions (see Fig. 2).

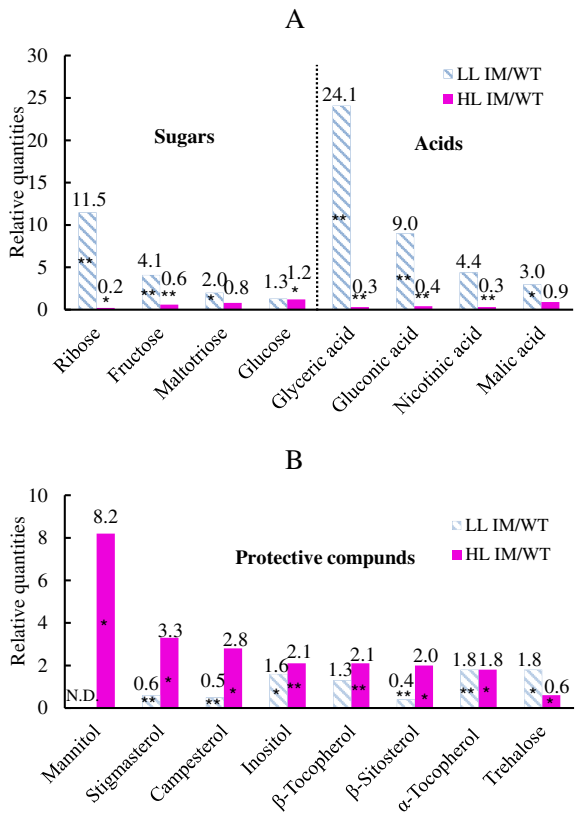

Fig. 7. Comparison of key metabolites for (A) carbon metabolism and (B) oxidative stress protection for IM and WT cultures grown in TAP medium, sampled during the exponential phase under fluorescent light of two different intensities: low light (LL, 20-μmol photons m^{-2} s^{-1}) and high light (HL, 640 μmol photons m^{-2} s^{-1}) conditions. Relative quantities were calculated as the ratio of metabolite levels in IM cells to the levels in WT cells. Three biological replicates and three analytical replicates were averaged in this analysis ($n = 9$). Statistically significant metabolite differences are denoted with a "*" ($p < 0.05$) or "**" ($p < 0.01$) in *t*-test. N.D. indicates not detected.

Another interesting observation is that, when cultivated under high light conditions, IM cells showed much higher levels of compounds involved in oxidative stress protection compared to WT cells. These compounds include osmolytes, antioxidants (mannitol [68,69], inositol [70,71], β-tocopherol [72,73]) and sterols (stigmasterol [74], campesterol [74] and beta-sitosterol [75,76]), all of which have protective function against various environmental stresses. We postulate that the up-regulation of these protective compounds in IM cells could be a metabolic response to compensate for the defects of phototaxis and photoshock response in IM cells, which were inherited from the parent KO mutant. These protective compounds may have helped the IM cells to maintain their photosynthetic capacity and may have contributed to its higher rate of O_2 evolution under high light conditions. Some other potentially beneficial metabolites found to be up-regulated in IM cells include plant hormones like salicylic acid [77,78] and gibberellic acid [79], which have been previously reported to increase photosynthetic efficiencies and promote growth in many algal species including *Chlorella vulgaris* and *C. reinhardtii* [80,81].

4. Discussion

4.1. Phototaxis behavior

Our results (Section 3.1; and Supplementary material) show that the phototaxis defects in KO cells are conserved in the IM cells. This was to be expected, since the integration of exogenous DNA in Chlamydomonas cells by insertional mutagenesis (as used to create

the progenitor KO strain) is usually associated with deletion of part of the chromosome at the insertion site, and therefore, it is very unlikely that any subsequent mutation would restore the deleted gene in its original form (see [28] for additional details).

4.2. Cell growth under different light intensities

As seen in Fig. 2, and as expected, all of the strains had a lower maximum biomass production when grown in low light (10–20 μmol photons m^{-2} s^{-1}), compared to high light (640 μmol photons m^{-2} s^{-1}) growth conditions. This is obvious because of more energy input, without any significant amount of photoinhibition [82]. Further, Ballottari el al. [83] have shown that high light conditions result in more Rubisco (ribulose−1,5-bisphosphate carboxylase/oxygenase), the key enzyme of the Calvin–Benson cycle, than at low light. Moreover, in *C. reinhardtii* cells grown photoautotrophically under high light, a decrease in the ratio of PSI/PSII (due to a decrease in PSI), and an increase in Cyt b6/f and ATP synthase have been observed [59] (see Fig. 1).

The growth experiment also showed that, under very low light, and under mixotrophic conditions, the IM strain had a very clear advantage compared to WT and KO, (i.e., 27% increased dry biomass; see Fig. 2A). It is well-known that in *C. reinhardtii* cells grown under mixotrophic conditions, both photosynthetic assimilation of inorganic carbon and heterotrophic assimilation of acetate contribute to biomass production. However, we note that the ability of acetate to induce isocitrate lyase, the key glyoxylate cycle enzyme necessary for its utilization, is attenuated in the presence of light and inorganic carbon, so that acetate assimilation could contribute more to biomass production than photosynthesis under lower irradiance. We note that Heifetz et al. [84] have shown that the photosynthetic fraction of carbon biomass of Chlamydomonas can be less than 3% under low light conditions (<25 μmol photons m^{-2} s^{-1}) when cultivated on solid medium. Thus, we suggest that an enhanced acetate assimilation in the IM strain may be one of the most important reasons for the better biomass production by IM in comparison to WT and KO strains. Indeed, as shown in Fig. 2D, IM cells, grown under 10 μmol photons m^{-2} s^{-1}, completely lost their advantage in the absence of acetate (grown in HSM medium), while WT cells showed an increased biomass production compared to IM (by 52%) and KO (by 67%). It is highly likely that the results obtained under photoautotrophic conditions may be due to a higher photosynthesis capacity in the WT strain in the absence of acetate, since acetate is known to affect negatively the photosynthetic activity in Chlamydomonas [84].

From the perspective of large-scale algal biofuel production, the growth of algae in the presence of organic carbon is highly important, especially to facilitate integration with wastewater treatment systems, as discussed earlier. Therefore, we consider it to be very important to characterize specialized strains of algae, such as our Chlamydomonas IM mutant, which can enhance biomass production in mixotrophic wastewater applications, which then supports the goal of using wastewater for large-scale algal cultivation.

4.3. Oxygen evolution

We note that results of oxygen measurements, as presented in Fig. 3, cannot be exactly correlated with the growth data in both mixotrophic and photoautotrophic conditions, since the algae were cultured under different light conditions (60 versus 10–20 μmol photons m^{-2} s^{-1}). Moreover, rates of O_2 evolution cannot always be strictly correlated with growth rates or biomass productivity in Chlamydomonas mutants, as is already known [17,85,86]. Even so, oxygen evolution is an important product of photosynthesis, and our results show significant differences for both IM and KO cells in comparison to the WT cells, as was consistently observed when cells were exposed to a wide range of light intensity levels during these tests.

4.4. Fluorescence based measurements

4.4.1. The fast chlorophyll fluorescence transient

C. reinhardtii cells, grown under low light (20 μmol photons m^{-2} s^{-1}), showed quite similar fast Chl *a* fluorescence transient curves (Fig. 4A) among the three strains, and therefore fluorescence parameters also had similar values (see Table 2). However, there were subtle differences: the IM strain had a slightly higher I level (Fig. 4A and C). Usually, the J–I phase is correlated with the redox status of the PQ-pool, which typically has 6–12 PQ molecules per PSII that shuttle electrons between PSII and PSI via cytochrome b6/f [87,88] (see Fig. 1, and a discussion of the evolution of the Z-scheme of electron transport by Govindjee and Björn [89]). The increased I level observed in the IM cells, compared to KO and WT cells, suggests a potentially slower oxidation rate of plastoquinol (PQH2) by PSI due possibly to a decreased PSI/PSII ratio in the IM cells (see discussion in Stirbet et al. [57]; Oukarroum et al. [52]; and Ceppi et al. [53]). Further, the IM strain showed higher F_v/F_m and F_v/F_o ratios compared to WT and KO strains, which may indicate a slightly better photosynthetic capacity (CO_2 fixation). However, considering all the data, reported in this paper, we suggest that other processes besides photosynthesis must have contributed to the increased growth performance observed in the IM mutant cells grown under a light intensity of 10 μmol photons m^{-2} s^{-1} (see Fig. 2A). Indeed, as discussed earlier, data on growth in HSM medium, without acetate and under this low light intensity, suggest that the IM advantage was most likely due to enhanced acetate assimilation compared to KO and WT.

In samples grown under high light (640 μmol photons m^{-2} s^{-1}), we observed clear differences in fast Chl fluorescence transient curves (Fig. 4B and D), and their respective fluorescence parameters (Table 2). All these samples had lower F_m, F_v/F_m, F_v/F_o, and OJ rise initial slopes, compared to those grown under low light, which may be partially due to photoinhibition. However, for KO cells, the initial slope of the OJ rise, as well as both F_o and F_m had much lower values than in any other sample, which may indicate a low PSII excitation cross section [34] and low fluorescence state; thus we propose that this sample likely had a State 1 to State 2 transition (high to low fluorescence) in darkness, which has also been observed under similar conditions by Allorent et al. [58].

4.4.2. The slow chlorophyll fluorescence transient

Kana et al. [62] have proposed that the S to M fluorescence rise observed under certain conditions in the slow (seconds to minutes) Chl fluorescence transient may be used to evaluate regulatory mechanisms such as state changes in cyanobacteria; also see Kodru et al. [63] for the same conclusion in Chlamydomonas. We note that state changes (i.e., State 1 ↔ State 2) are regulatory mechanisms that optimize photosynthesis by adjusting the amount of excitation energy delivered by antenna pigments to PSII and PSI reaction centers under changing light regimes and/or metabolic needs [90–94]. In Chlamydomonas, state changes are different than in plants because they can involve detachment of a higher proportion of LHCII trimers from the PSII antenna (70–80% versus 10–15% in plants, see Delosme et al. [95]). However, only ~10% of these are actually incorporated in PSI antenna, and the rest form arrays that quench the Chl *a* excited state [96,97]. Therefore, in Chlamydomonas, the State 1 to State 2 transition seems to play an important role for short term (minutes) protection under high light conditions, which may compensate for the much slower (hours) non-photochemical (NPQ) response in these algae as compared to plants [58,97,98]. Furthermore, state changes in Chlamydomonas were also found to coincide with changes in the ratio between cyclic and linear electron flow, and thus, the ATP/ADP ratio in cells [94,99].

Fig. 5 shows that the SM rise in the slow Chl fluorescence transient of the IM cells, grown in TAP medium, is absent. We speculate that similar to the *RpaC*$^{-}$ mutant of *Synechocystis* PCC6803 [62] and *stt7* mutant of *C. reinhardtii* [63] (as mentioned earlier), the IM strain may have a reduced capacity to perform state changes under our experimental

conditions, even if other processes may also contribute to the SM phase (see a discussion in Stirbet et al. [57]). This hypothesis is also supported by the results for NPQ kinetics in Chlamydomonas cells as discussed below.

Since the IM mutant is not yet genetically characterized, we do not have a clear explanation for its possible lower ability to perform state changes, as suggested by our fluorescence measurements. This may be due to a mutation affecting genes directly related to state changes, or it could be related to factors that influence the PQ pool redox state, which regulates the induction of state changes via Cyt b6f (see e.g., [63] for further discussion). However, our growth experiments under photoautotrophic conditions without acetate present showed that the biomass production in IM and KO cells grown under low light (10 μmol photons m^{-2} s^{-1}) is lower than in the WT cells. Thus, we propose that an enhanced acetate metabolism (that keeps the PQ pool in a more reduced state; see Fig. 1) may be the most likely cause for a reduced capacity of the IM cells to perform state transitions.

4.4.3. Non-photochemical quenching kinetics

Several types of NPQ have been identified [see e.g., [100–102] for a background and mechanisms of NPQ in Chlamydomonas], each one characterized by a particular kinetic behavior: pH-dependent (qE) [103–105], state change-dependent (qT) [90], and photoinhibition-dependent (qI) [106]. However, we note that qT in most plants is not a true NPQ process because it does not involve changes in the rate constants of the de-excitation processes of singlet excited Chl *a*, but rather only changes in the antenna size of the two photosystems [90,93]. However, in Chlamydomonas, during State 1 to State 2 transition, part of mobile phosphorylated LHCII trimers was shown to form arrays in the membrane, in which nonphotochemical quenching (of qE type) takes place [107,108], as mentioned above.

The qE quenching is the most rapid component of NPQ and is triggered by a pH gradient (ΔpH) that builds-up across the thylakoid membrane (see Fig. 1). Therefore, qE is affected by all processes that influence ΔpH, including ATP synthase activity, the linear and PSI-dependent cyclic electron transport flow, and ATP and NADPH consumption by the Calvin–Benson cycle (see Fig. 1). However, in contrast to higher plants, qE in Chlamydomonas is not dependent on the presence of PsbS [109], but on other proteins, such as Light-Harvesting Complex Stress-Related proteins (e.g., LhcSR1 and LhcSR3), which can sense pH changes and, unlike PsbS, can also bind pigments (Chl *a* and *b*, violaxanthin, zeaxanthin, and lutein) [110–112].

We note that in contrast to higher plants, even under saturating light, Chlamydomonas cells have a higher contribution of state 1 to state 2 transition and photoinhibition, rather than qE, for the lowering of fluorescence intensity, independent of the growth light intensity [113].

The results of PAM experiments showed complex NPQ kinetics, both in samples grown under low light and high light conditions (Fig. 6C and D). Specifically, our results show that among the three strains of *C. reinhardtii* cells, grown in low light, the NPQ increased to the highest level in IM (most likely due to the qE component): the NPQ developed by the IM cells at the end of the illumination with actinic light was twice as high as NPQ in WT and KO strains (Fig. 6C), and IM had a faster and more complete recovery in darkness. We suggest that the higher NPQ level observed in IM cells is mainly related to its capacity to induce an increased ΔpH across the thylakoid membrane [93], which is most probably due to its enhanced acetate metabolism compared to WT and KO cells. Indeed, the presence of acetate, which increases the production of reducing power in the mitochondria (see Fig. 1), has been known to have an impact on the redox state of plastoquinones [114]. Surprisingly, we also observed that after the actinic light was switched off, the NPQ continued to increase for 1–2 min in all these samples, before dark relaxation took place. However, in IM cells the NPQ increase finished much sooner and was very small compared to that in the WT and KO cells, which more than doubled their NPQ values reached during actinic illumination (see Fig. 6C). A possible explanation of NPQ increase taking place after the actinic light was turned off, may be the induction of a state transition, as noted by Allorent et al. [58]; indeed, they had also measured an increase in NPQ during the dark relaxation period in WT cells of *C. reinhardtii*, which was correlated with an increase in LHCII phosphorylation, and thus to a State 1 to State 2 transition. Further, as shown in Fig. 6C, at the end of the dark relaxation period, the IM cells attained a lower NPQ level than WT and KO, which implies that they might be better protected against photoinhibition.

In cells grown under high light, KO reached a higher NPQ level during actinic illumination than WT and IM cells. However, in all likelihood, a large part of this NPQ in WT and KO cells was not of the qE type, since their dark relaxation was only partial, and we know that qE is fully reversible in darkness; in contrast, the NPQ recovered completely in the IM cells. Since qE is dependent on the accumulation of LhcSR proteins, these results suggest that Chlamydomonas cells grown under high light conditions may have higher levels of LhcSR proteins than those grown under low light, which offers a higher degree of photoprotection [96,111]. Other explanations are also possible for higher NPQ (that is lower fluorescence), such as quenching by higher [H+] due to increased ΔpH (see e.g., Ref. [84]), which in IM strain, as explained earlier, can be the result of its increased acetate metabolism. In samples grown under high light, we also observed a transient NPQ increase after the actinic light was turned off, but it was much smaller than in samples grown in low light, and mainly in the WT cells. The fact that the NPQ increase during the dark relaxation period was much lower in IM cells (both in cells grown in low and high light conditions; see Fig. 6C and D) supports our suggestion that IM cells may have reduced state transition capacity in comparison to WT and KO cells. As discussed above, since the biomass advantage of the IM cells, grown in low light in TAP medium, was lost in HSM medium, when WT cells showed a higher biomass production than IM and KO cells (Fig. 2D), we suggest that the reduced capacity for state changes of the IM strain, if it exists, is probably due to a mutation enhancing acetate related cellular processes.

It is important to note that in WT cells grown in high light (and to a lesser extent for cells grown in low light), fluorescence showed a transient increase after ~100 s actinic illumination (Fig. 6), similar (even if smaller) to the SM rise shown in Fig. 5. Such a transient fluorescence increase was also reported by Allorent et al. [58] during actinic illumination in WT Chlamydomonas cells that were initially in State 2; this fluorescence increase was assigned to a State 2 to State 1 transition, because it was absent in the stt7–9 mutant (locked in State 1); further, the phosphorylation level of LHCII was shown to decrease upon illumination. Since this transient fluorescence recovery, and the SM rise observed in Fig. 5, are related phenomena, our results, as well as those presented by Allorent et al. [58], strongly support our hypothesis that SM rise in the OJIPSMT transient reflects a State 2 to State 1 change.

In summary, results of our NPQ kinetics experiments may be interpreted to mean that WT cells might have undergone a State 2 to State 1 transition during actinic illumination, and a State 2 to State 1 transition after the actinic light was switched off. As compared to WT and KO, IM cells showed the highest NPQ level at the end of illumination; this was especially true when cells were grown under low light, and are characterized by fast recovery of NPQ in darkness. Further, these IM cells seem to be better protected against photoinhibition (especially when grown under high light), but are probably less capable of undergoing state transitions, compared to WT and KO cells. We assume that these differences between the IM and KO and WT strains may have their origin in its enhanced acetate assimilation in IM, as suggested by comparing the growth curves under mixotrophic and photoautotrophic conditions (see Section 4.2).

4.5. Metabolite profiling

The metabolite profiling results of the IM strain showed some advantages over the WT strain in terms of metabolites related to carbon

metabolism when grown under low light conditions, which, as suggested earlier, may be related to better acetate assimilation. Under high light conditions, the IM advantages changed to enhanced production of metabolites that mitigate oxidative stress. However, the signaling and regulatory mechanisms of the IM strain mutation leading to these potentially beneficial alterations in carbon metabolism and stress responses are unclear. In addition, it is unknown at this time whether these metabolite effects are a result of the knocked-out gene in the KO parent strain, or if they are a result of further mutations in the IM strain. Further molecular studies are necessary to identify the genetic basis of the differences observed in this study. In addition, global gene expression patterns, when available, would provide useful information for linking the function of the metabolic network with gene expression.

5. Concluding remarks

Our growth curve data suggest that the IM cells are more efficient than the WT cells in terms of biomass production when grown under low light and mixotrophic conditions, which is potentially a very valuable feature for algal biofuel production. Mass algal production involves optically dense cultures, where most of the cultivation reactor space is likely to be light limited, which would normally result in reduced or arrested cell growth. For example, one previous study with dense cultures (1 g/l), found that 80–95% of the light path was severely light limited [9]. In cases where light is limiting, it would likely be advantageous to use algal strains, such as the IM cells reported here, that have improved biomass production under low light conditions. This feature may also make the IM strain a good candidate for outdoor algae cultivation systems that depend on natural light and experience highly dynamic incident photon irradiance conditions as a result of variations in solar elevation, cloud cover, and even rain. Low light requirements for photosynthesis also allow a longer period of biomass production and therefore an improved overall biomass production.

It is interesting to note that, under 60 μmol photons m^{-2} s^{-1} in mixotrophic cultivation condition, although both KO and IM cells show higher O_2 evolution rate than WT cells, only IM cells showed an obvious advantage in biomass production under low light conditions. Generally, oxygen evolution rate can be used as an indicator of photosynthetic capacity because oxidation of water provides the primary source of reducing equivalent (water derived electrons and protons) and, ultimately ATP, which is used later for the conversion of CO_2 into biomass [115]. Therefore, high O_2 evolution rates would normally be correlated with high photoautotrophic biomass production in algal cells. However, when some other metabolic process downstream of the light reactions (e.g., dark reactions, starch synthesis or cell division) act as a rate limiting step, the O_2 evolution rate may not directly or accurately reflect the growth rate/biomass productivity. Several other studies [17,85,86] have reported *C. reinhardtii* mutants with reduced or increased O_2 evolution rate but unaffected biomass growth compared to wild type cells. However, results obtained in growth and Chl *a* fluorescence experiments suggest that it is quite possible that the differences between the two mutant strains (KO and IM) and the WT when grown under very low light are mainly related to their dissimilarities in other cellular processes such as acetate assimilation, starch synthesis and consumption, or regulation of cell division. The involvement of these mechanisms is to be expected, as the IM cells display better cell growth primarily under low light, and during the exponential growth phase, when the cell division rate and biomass production rate are high.

Highlights of our research

We have discovered that a spontaneous mutant (that we refer to as IM) of the green alga *C. reinhardtii* (that has kept the phototaxis defects of its progenitor KO) exhibits certain unique biophysical and biochemical characteristics, which are potentially advantageous for biofuel production systems in comparison to its progenitor KO strain and WT cells. When cultivated mixotrophically, IM cells have increased biomass production (5%–27% higher than in WT and KO) under low light intensities (10–20 μmol photons m^{-2} s^{-1}), but they do not show any productivity advantages under high light conditions (640 μmol photons m^{-2} s^{-1}). However, IM did not show this advantage when cultivated photoautotrophically under 10 μmol photons m^{-2} s^{-1} light intensity, which suggests that the acetate metabolism is enhanced in this mutant. Both IM and KO cells grown under 60 μmol photons m^{-2} s^{-1} showed approximately 1.5 fold increase in O_2 evolution rate over a large range of light intensities (20–800 μmol photons m^{-2} s^{-1}) as compared to WT cells. Slow chlorophyll *a* fluorescence transient, the SMT phase, indicates that the IM cells grown under low light intensity (20 μmol photons m^{-2} s^{-1}) may be less able to undergo state changes when grown (and/or re-suspended) in TAP medium; however, we speculate that they can, perhaps, develop a higher pH-dependent non-photochemical quenching of the Chl *a* excited states (qE) than the WT and KO cells, as affected by the presence of acetate. Overall, these results indicate that IM cells are advantageous in biomass production under low light and mixotrophic conditions, which is potentially a valuable feature for large-scale algal biofuel production, where light-limiting reactor conditions are expected. Additionally, in comparison to WT cells, metabolite profiling analysis showed that the IM cells had higher concentrations of important soluble carbohydrates and organic acids that are closely related to carbon metabolism when cultivated under low light. Under high light, IM did not have increased carbon metabolites, but higher levels of metabolites that can protect against oxidative damage (see the above discussion and Fig. 7).

These unique attributes are promising and suggest that further molecular, physiological and metabolic studies on these mutants are justified to help better elucidate these distinctive characteristics. Ultimately, metabolic and genetic engineering could be used to transfer desirable features into other algae to improve the efficiency of algal biofuel production systems [5,116], as well as other algal biochemical manufacturing platforms (such as recombinant proteins, including various antioxidants, hormones) for industrial, nutritional and medical uses [117, 118].

Acknowledgments

We thank Reto J. Strasser who provided us the Handy PEA instrument and the Biolyzer software. We also thank Richard Sayre and Sangeeta Negi who provided equipment and technical support for oxygen evolution measurements and analysis. In addition, we thank Gregory Pazour for his help with the phototaxis experiment. We acknowledge support from the Clean Energy Education Initiative of the Graduate College at the University of Illinois at Urbana–Champaign. Govindjee thanks Jeff Haas and all the staff at the Office of Information Technology (Life Sciences) at the University of Illinois at Urbana–Champaign for their support in Information Technology.

Appendix A. Supplementary data

Supplementary data to this article can be found online at http://dx.doi.org/10.1016/j.algal.2015.06.001.

References

[1] Y. Chisti, Biodiesel from microalgae, Biotechnol. Adv. 25 (3) (2007) 294–306.
[2] R. Sayre, Microalgae: the potential for carbon capture, Bioscience 60 (9) (2010) 722–727.
[3] M.L. Ghirardi, L. Zhang, J.W. Lee, T. Flynn, M. Seibert, E. Greenbaum, A. Melis, Microalgae: a green source of renewable H_2, Trends Biotechnol. 18 (12) (2000) 506–511.
[4] M.L. Ghirardi, Photobiological H_2 production: theoretical maximum light conversion efficiency and strategies to achieve it, ECS Trans. 50 (49) (2013) 47–50.
[5] A.G. Dubini Maria, Engineering photosynthetic organisms for the production of biohydrogen, Photosynth. Res. 123 (3) (2015) 241–253.

[6] E.M. Trentacoste, A.M. Martinez, T. Zenk, The place of algae in agriculture: policies for algal biomass production, Photosynth. Res. 123 (3) (2015) 305–315.
[7] U.S. DOE, National Algal Biofuels Technology Roadmap, US Department of Energy, Office of Energy Efficiency and Renewable Energy, Biomass Program, 2010.
[8] J. Sheehan, T. Dunahay, J. Benemann, P. Roessler, A Look Back at the U.S. Department of Energy's Aquatic Species Program: Biodiesel from Algae, National Renewable Energy Laboratory, Golden, Colorado, 1998.
[9] P.J.L.B. Williams, L.M.L. Laurens, Microalgae as biodiesel biomass feedstocks: review analysis of the biochemistry, energetics economics, Energy Environ. Sci. 3 (5) (2010) 554.
[10] J. Ogbonna, H. Tanaka, Light requirement and photosynthetic cell cultivation — development of processes for efficient light utilization in photobioreactors, J. Appl. Phycol. 12 (3-5) (2000) 207–218.
[11] N. Adir, H. Zer, S. Shochat, I. Ohad, Photoinhibition — a historical perspective, Photosynth. Res. 76 (1-3) (2003) 343–370.
[12] A. Melis, Solar energy conversion efficiencies in photosynthesis: minimizing the chlorophyll antennae to maximize efficiency, Plant Sci. 177 (4) (2009) 272–280.
[13] J. Polle, S. Kanakagiri, E. Jin, T. Masuda, A. Melis, Truncated chlorophyll antenna size of the photosystems — a practical method to improve microalgal productivity and hydrogen production in mass culture, Int. J. Hydrog. Energy 27 (11-12) (2002) 1257–1264.
[14] J. Polle, S. Kanakagiri, A. Melis, tla1, a DNA insertional transformant of the green alga *Chlamydomonas reinhardtii* with a truncated light-harvesting chlorophyll antenna size, Planta 217 (1) (2003) 49–59.
[15] J. Beckmann, F. Lehr, G. Finazzi, B. Hankamer, C. Posten, L. Wobbe, Improvement of light to biomass conversion by de-regulation of light-harvesting protein translation in *Chlamydomonas reinhardtii*, J. Biotechnol. 142 (1) (2009) 70–77.
[16] S.N. Kosourov, M.L. Ghirardi, M. Seibert, A truncated antenna mutant of *Chlamydomonas reinhardtii* can produce more hydrogen than the parental strain, Int. J. Hydrog. Energy 36 (3) (2011) 2044–2048.
[17] Z. Perrine, S. Negi, R.T. Sayre, Optimization of photosynthetic light energy utilization by microalgae, Algal Res. 1 (2) (2012) 134–142.
[18] National Research Council, Sustainable Development of Algal Biofuels, The National Academies Press, Washington, DC, 2012.
[19] T.J. Lundquist, I.C. Woertz, N.W.T. Quinn, J.R. Benemann, A Realistic Technology and Engineering Assessment of Algae Biofuel Production, Energy Biosciences Institute, 2010. (178 pages).
[20] E.H. Harris, Chlamydomonas as a model organism, Annu. Rev. Plant Biol. 52 (1) (2001) 363–406.
[21] A. Grossman, Acclimation of *Chlamydomonas reinhardtii* to its nutrient environment, Protist 151 (3) (2000) 201–224.
[22] A. Grossman, H. Takahashi, Macronutrient utilization by photosynthetic eukaryotes and the fabric of interactions, Annu. Rev. Plant Biol. 52 (1) (2001) 163–210.
[23] J. Rochaix, *Chlamydomonas reinhardtii* as the photosynthetic yeast, Annu. Rev. Genet. 29 (1) (1995) 209–230.
[24] P. Altimari, F. Di Caprio, L. Toro, A.L. Capriotti, F. Pagnanelli, Hydrogen photoproduction by mixotrophic cultivation of *Chlamydomonas reinhardtii*: interaction between organic carbon and nitrogen, Chem. Eng. Trans. 38 (2014) 199–204.
[25] N.R. Boyle, J.A. Morgan, Flux balance analysis of primary metabolism in *Chlamydomonas reinhardtii*, BMC Syst. Biol. 3 (2009) 4, http://dx.doi.org/10.1186/1752-0509-3-4.
[26] E. Spijkerman, Phosphorus acquisition by *Chlamydomonas acidophila* under autotrophic and osmo-mixotrophic growth conditions, J. Exp. Bot. 58 (15-16) (2007) 4195–4202.
[27] J. Rochaix, M. Goldschmidt-Clermont, S. Merchant, The molecular biology of chloroplasts and mitochondria in Chlamydomonas, Advances in Photosynthesis and Respirationvol. 7, Springer, Dordrecht, 1998.
[28] G. Pazour, O. Sineshchekov, G. Witman, Mutational analysis of the phototransduction pathway of *Chlamydomonas reinhardtii*, J. Cell Biol. 131 (2) (1995) 427–440.
[29] J. Alric, Cyclic electron flow around photosystem I in unicellular green algae, Photosynth. Res. 106 (1-2) (2010) 47–56.
[30] M.H. Hoefnagel, O.K. Atkin, J.T. Wiskich, Interdependence between chloroplasts and mitochondria in the light and the dark, Biochim. Biophys. Acta 1366 (3) (1998) 235–255.
[31] F. Mus, L. Cournac, V. Cardettini, A. Caruana, G. Peltier, Inhibitor studies on non-photochemical plastoquinone reduction and H_2 photoproduction in *Chlamydomonas reinhardtii*, Biochim. Biophys. Acta 1708 (3) (2005) 322–332.
[32] Y. Zhou, C.L. Schideman, S.I. Rupassara Govindjee, M.J. Seufferheld, Improving the photosynthetic productivity and light utilization in algal biofuel systems: metabolic and physiological characterization of a potentially advantageous mutant of *Chlamydomonas reinhardtii*, in: C. Lu (Ed.), Photosynthesis: Research for Food, Fuel and Future — 15th International Conference on Photosynthesis, Symposium 16–20, Zhejiang University Press, Springer-Verlag GmbH, Beijing, China 2012, pp. 529–533.
[33] L.S. Clesceri, A.E. Greenberg, D.E. Andrew, Standard Methods for the Examination of Water and Wastewater, American Public Health Association, New York, 1999.
[34] R.J. Strasser, A. Srivastava, M. Tsimilli-Michael, The fluorescence transient as a tool to characterize and screen photosynthetic samples, in: M. Yunus, U. Pathre, P. Mohanty (Eds.), Probing Photosynthesis: Mechanisms, Regulation, and Adaptation, Taylor & Francis, London, New York 2000, pp. 443–480.
[35] R.J. Strasser, M. Tsimilli-Michael, A. Srivastava, Analysis of the chlorophyll a fluorescence transient, in: G.C. Papageorgiou, Govindjee (Eds.), Chlorophyll a Fluorescence: A Signature of Photosynthesis, Advances in Photosynthesis and Respiration, vol. 19, Springer, Dordrecht 2004, pp. 321–362.
[36] A. Stirbet, Govindjee, On the relation between the Kautsky effect (chlorophyll a fluorescence induction) and photosystem II: basics and applications of the OJIP fluorescence transient, J. Photochem. Photobiol. B Biol. 104 (1-2) (2011) 236–257.
[37] M. Tsimilli-Michael, R.J. Strasser, In vivo assessment of stress impact on plant's vitality: applications in detecting and evaluating the beneficial role of mycorrhization on host plants, in: A. Varma (Ed.), Mycorrhiza: State of the Art. Genetics and Molecular Biology, Eco-function, Biotechnology, Eco-physiology, Structure and Systematics, Springer, Berlin, Heidelberg 2008, pp. 679–703.
[38] Govindjee, Sixty-three years since Kautsky: chlorophyll a fluorescence, Aust. J. Plant Physiol. 22 (2) (1995) 131–160.
[39] J. Toepel, M. Gilbert, C. Wilhelm, Can chlorophyll-a in-vivo fluorescence be used for quantification of carbon-based primary production in absolute terms? Arch. Hydrobiol. 160 (4) (2004) 515–526.
[40] K. Oxborough, N.R. Baker, Resolving chlorophyll a fluorescence images of photosynthetic efficiency into photochemical and non-photochemical components — calculation of qP and Fv′/Fm′ without measuring Fo′, Photosynth. Res. 54 (2) (1997) 135–142.
[41] B. Demmig-Adams, G. Garab, W. Adams III, Govindjee (Eds.), Non-photochemical Quenching and Energy Dissipation in Plants, Algae and Cyanobacteria, Advances in Photosynthesis and Respiration Including Bioenergy and Related Processes, vol. 40, Springer, Dordrecht, 2014.
[42] O. Fiehn, J. Kopka, R. Trethewey, L. Willmitzer, Identification of uncommon plant metabolites based on calculation of elemental compositions using gas chromatography and quadrupole mass spectrometry, Anal. Chem. 72 (15) (2000) 3573–3580.
[43] J. Lisec, N. Schauer, J. Kopka, L. Willmitzer, A. Fernie, Gas chromatography mass spectrometry-based metabolite profiling in plants, Nat. Protoc. 1 (1) (2006) 387–396.
[44] S.I. Rupassara, Metabolite Profiling of Leaves and Vascular Exudates of Soybean Grown Under Free-Air Concentration Enrichment(PhD) University of Illinois at Urbana–Champaign, Urbana, IL, 2008.
[45] M. Keller, Photosynthesis and respiration, in: M. Keller (Ed.), The Science of Grapevines: Anatomy and Physiology, Academic Press, San Diego 2010, pp. 107–123.
[46] K. Maxwell, G. Johnson, Chlorophyll fluorescence — a practical guide, J. Exp. Bot. 51 (345) (2000) 659–668.
[47] G.C. Papageorgiou, Govindjee (Eds.), Chlorophyll a Fluorescence: A Signature of Photosynthesis, Advances in Photosynthesis and Respiration, vol. 19, Springer, Dordrecht Maxwell, MA, 2004.
[48] N.R. Baker, Chlorophyll fluorescence: a probe of photosynthesis in vivo, Annu. Rev. Plant Biol. 59 (2008) 89–113.
[49] H.M. Kalaji, V. Goltsev, K. Bosa, S.I. Allakhverdiev, R.J. Strasser, Govindjee, Experimental in vivo measurements of light emission in plants: a perspective dedicated to David Walker, Photosynth. Res. 114 (2) (2012) 69–96.
[50] R.J. Strasser, Govindjee, The Fo and the OJIP fluorescence rise in higher plants and algae, in: J.H. Argyroudi-Akoyunoglou (Ed.), Regulation of Chloroplast Biogenesis, Plenum Press, New York 1991, pp. 423–426.
[51] R.J. Strasser, M. Tsimilli-Michael, D. Dangre, M. Rai, Biophysical phenomics reveals functional building blocks of plants systems biology: a case study for the evaluation of the impact of mycorrhization with *Piriformospora indica*, in: A. Varma, R. Oelmüller (Eds.),Advanced Techniques in Soil Microbiology, Soil Biology, vol. 11, Springer, Berlin, Heidelberg 2007, pp. 319–341.
[52] A. Oukarroum, G. Schansker, R.J. Strasser, Drought stress effects on photosystem I content and photosystem II thermotolerance analyzed using Chl *a* fluorescence kinetics in barley varieties differing in their drought tolerance, Physiol. Plant. 137 (2) (2009) 188–199.
[53] M.G. Ceppi, A. Oukarroum, N. Çiçek, R.J. Strasser, G. Schansker, The IP amplitude of the fluorescence rise OJIP is sensitive to changes in the photosystem I content of leaves: a study on plants exposed to magnesium and sulfate deficiencies, drought stress and salt stress, Physiol. Plant. 144 (3) (2012) 277–288.
[54] M.A. Yusuf, D. Kumar, R. Rajwanshi, R.J. Strasser, M. Tsimilli-Michael, N.B. Sarin Govindjee, Overexpression of γ-tocopherol methyl transferase gene in transgenic *Brassica juncea* plants alleviates abiotic stress: physiological and chlorophyll a fluorescence measurements, Biochim. Biophys. Acta 1797 (8) (2010) 1428–1438.
[55] W.L. Butler, M. Kitajima, Fluorescence quenching in photosystem II of chloroplasts, Biochim. Biophys. Acta 376 (1) (1975) 116–125.
[56] Govindjee, Chlorophyll a fluorescence: a bit of basics and history, in: G.C. Papageorgiou, Govindjee (Eds.), Chlorophyll a Fluorescence: A Signature of Photosynthesis, Advances in Photosynthesis and Respiration, vol. 19, Springer, Dordrecht 2004, pp. 1–41.
[57] A. Stirbet, G. Riznichenko, A. Rubin, Govindjee, Modeling chlorophyll a fluorescence transient: relation to photosynthesis, Biochem. Mosc. 79 (4) (2014) 291–323.
[58] G. Allorent, R. Tokutsu, T. Roach, G. Peers, P. Cardol, J. Girard-Bascou, D. Seigneurin-Berny, D. Petroutsos, M. Kuntz, C. Breyton, F. Franck, F.A. Wollman, K.K. Niyogi, A. Krieger-Liszkay, J. Minagawa, G. Finazzi, A dual strategy to cope with high light in *Chlamydomonas reinhardtii*, Plant Cell 25 (2) (2013) 545–557.
[59] G. Bonente, S. Pippa, S. Castellano, R. Bassi, M. Ballottari, Acclimation of *Chlamydomonas reinhardtii* to different growth irradiances, J. Biol. Chem. 287 (8) (2012) 5833–5847.
[60] G. Papageorgiou, Govindjee, Light-induced changes in the fluorescence yield of chlorophyll a in vivo. I. *Anacystis nidulans*, Biophys. J. 8 (11) (1968) 1299–1315.
[61] G. Papageorgiou, Govindjee, Light-induced changes in the fluorescence yield of chlorophyll a in vivo. II. *Chlorella pyrenoidosa*, Biophys. J. 8 (11) (1968) 1316–1328.
[62] R. Kaňa, E. Kotabová, O. Komárek, B. Šedivá, G.C. Papageorgiou, Govindjee, O. Prášil, The slow S to M fluorescence rise in cyanobacteria is due to a state 2 to state 1 transition, Biochim. Biophys. Acta 1817 (8) (2012) 1237–1247.

[63] S. Kodru, T. Malavath, E. Devadasu, S. Nellaepalli, A. Stirbet, R. Subramanyam, Govindjee, The slow S to M rise of chlorophyll a fluorescence induction reflects transition from state 2 to state 1 in the green alga Chlamydomonas reinhardtii, Photosynth. Res. (2015)http://dx.doi.org/10.1007/s11120-015-0084-2.
[64] N. Depege, S. Bellafiore, J.D. Rochaix, Role of chloroplast protein kinase Stt7 in LHCII phosphorylation and state transition in Chlamydomonas, Science 299 (5612) (2003) 1572–1575.
[65] B. Demmig-Adams, W. Adams III, A.K. Mattoo (Eds.), Photoprotection, Photoinhibition, Gene Regulation, and Environment, Advances in Photosynthesis and Respiration, vol. 21, Springer, Dordrecht, 2006.
[66] M.D. Brooks, E.J. Sylak-Glassman, G.R. Fleming, K.K. Niyogi, A thioredoxin-like/beta-propeller protein maintains the efficiency of light harvesting in Arabidopsis, Proc. Natl. Acad. Sci. U. S. A. 110 (29) (2013) E2733–E2740.
[67] J. López-Bucio, M.F. Nieto-Jacobo, V. Ramírez-Rodríguez, L. Herrera-Estrella, Organic acid metabolism in plants: from adaptive physiology to transgenic varieties for cultivation in extreme soils, Plant Sci. 160 (1) (2000) 1–13.
[68] J.M.H. Stoop, J.D. Williamson, D.M. Pharr, Mannitol metabolism in plants: a method for coping with stress, Trends Plant Sci. 1 (5) (1996) 139–144.
[69] R. Voegele, M. Hahn, G. Lohaus, T. Link, I. Heiser, Possible roles for mannitol and mannitol dehydrogenase in the biotrophic plant pathogen *Uromyces fabae*, Plant Physiol. 137 (1) (2005) 190–198.
[70] F.A. Loewus, P.P.N. Murthy, Myo-inositol metabolism in plants, Plant Sci. 150 (1) (2000) 1–19.
[71] R. Valluru, W. Van den Ende, Myo-inositol and beyond — emerging networks under stress, Plant Sci. 181 (4) (2011) 387–400.
[72] A. Sirikhachornkit, J.W. Shin, I. Baroli, K.K. Niyogi, Replacement of α-tocopherol by β-tocopherol enhances resistance to photooxidative stress in a xanthophyll-deficient strain of *Chlamydomonas reinhardtii*, Eukaryot. Cell 8 (11) (2009) 1648–1657.
[73] H. Maeda, D. Della, Tocopherol functions in photosynthetic organisms, Curr. Opin. Plant Biol. 10 (3) (2007) 260–265.
[74] H. Schaller, The role of sterols in plant growth and development, Prog. Lipid Res. 42 (3) (2003) 163–175.
[75] U.K. Divi, P. Krishna, Brassinosteroid: a biotechnological target for enhancing crop yield and stress tolerance, New Biotechnol. 26 (3–4) (2009) 131–136.
[76] P. Benveniste, Biosynthesis and accumulation of sterols, Annu. Rev. Plant Biol. 55 (2004) 429–457.
[77] Q. Hayat, S. Hayat, M. Irfan, A. Ahmad, Effect of exogenous salicylic acid under changing environment: a review, Environ. Exp. Bot. 68 (1) (2010) 14–25.
[78] M. Vicente, J. Plasencia, Salicylic acid beyond defence: its role in plant growth and development, J. Exp. Bot. 62 (10) (2011) 3321–3338.
[79] A. Kadioglu, The effects of gibberellic acid on photosynthetic pigments and oxygen evolution in Chlamydomonas and Anacystis, Biol. Plant. 34 (1-2) (1992) 163–166.
[80] R. Czerpak, A. Bajguz, M. Gromek, G. Kozłowska, I. Nowak, Activity of salicylic acid on the growth and biochemism of *Chlorella vulgaris* Beijerinck, Acta Physiol. Plant. 24 (1) (2002) 45–52.
[81] A.M. Ismail, M.A. Abou Alhamd, H.R.M. Galal, F.A. Nasr-Eldeen, Modification of photosynthetic pigments, osmotic solutes and ions accumulation in chlorella vulgaris and wheat Cv. Sds-1 seedlings under the influence of NaCl with salicylic acids, Res. J. Bot. 6 (3) (2011) 100–111.
[82] N.R. Boyle, J.A. Morgan, Flux balance analysis of primary metabolism in *Chlamydomonas reinhardtii*, BMC Syst. Biol. 3 (1) (2009) 4.
[83] M. Ballottari, L. Dall'Osto, T. Morosinotto, R. Bassi, Contrasting behavior of higher plant photosystem I and II antenna systems during acclimation, J. Biol. Chem. 282 (12) (2007) 8947–8958.
[84] P.B. Heifetz, B. Forster, C.B. Osmond, L.J. Giles, J.E. Boynton, Effects of acetate on facultative autotrophy in *Chlamydomonas reinhardtii* assessed by photosynthetic measurements and stable isotope analyses, Plant Physiol. 122 (4) (2000) 1439–1445.
[85] B. Forster, C.B. Osmond, J.E. Boynton, N.W. Gillham, Mutants of *Chlamydomonas reinhardtii* resistant to very high light, J. Photochem. Photobiol. B 48 (2-3) (1999) 127–135.
[86] A. Lardans, B. Forster, O. Prasil, P. Falkowski, V. Sobolev, Biophysical, biochemical, and physiological characterization of *Chlamydomonas reinhardtii* mutants with amino acid substitutions at the Ala(251) residue in the D1 protein that result in varying levels of photosynthetic competence, J. Biol. Chem. 273 (18) (1998) 11082–11091.
[87] H. Kirchhoff, S. Horstmann, E. Weis, Control of the photosynthetic electron transport by PQ diffusion microdomains in thylakoids of higher plants, Biochim. Biophys. Acta 1459 (1) (2000) 148–168.
[88] A. Stirbet, Govindjee, Chlorophyll a fluorescence induction: a personal perspective of the thermal phase, the J–I–P rise, Photosynth. Res. 113 (1-3) (2012) 15–61.
[89] Govindjee, L.O. Björn, Dissecting oxygenic photosynthesis: the evolution of the "Z"-scheme for thylakoid reactions, in: S. Itoh, P. Mohanty, K.N. Guruprasad (Eds.), Photosynthesis: Overviews on Recent Progress & Future Perspective, I K International Publishing House, New Delhi, India 2012, pp. 1–27.
[90] J. Minagawa, State transitions—the molecular remodeling of photosynthetic supercomplexes that controls energy flow in the chloroplast, Biochim. Biophys. Acta 1807 (8) (2011) 897–905.
[91] N. Murata, Control of excitation transfer in photosynthesis I. Light-induced change of chlorophyll a fluoresence in *Porphyridium cruentum*, Biochim. Biophys. Acta 172 (2) (1969) 242–251.
[92] C. Bonaventura, J. Myers, Fluorescence and oxygen evolution from *Chlorella pyrenoidosa*, Biochim. Biophys. Acta 189 (3) (1969) 366–383.
[93] G.C. Papageorgiou, Govindjee, Photosystem II fluorescence: slow changes—scaling from the past, J. Photochem. Photobiol. B Biol. 104 (1) (2011) 258–270.
[94] J. Rochaix, Chlamydomonas, a model system for studying the assembly and dynamics of photosynthetic complexes, FEBS Lett. 529 (1) (2002) 34–38.
[95] R. Delosme, J. Olive, F. Wollman, Changes in light energy distribution upon state transitions: an in vivo photoacoustic study of the wild type and photosynthesis mutants from *Chlamydomonas reinhardtii*, Biochim. Biophys. Acta 1273 (2) (1996) 150–158.
[96] G. Nagy, R. Unnep, O. Zsiros, R. Tokutsu, K. Takizawa, L. Porcar, L. Moyet, D. Petroutsos, G. Garab, G. Finazzi, J. Minagawa, Chloroplast remodeling during state transitions in *Chlamydomonas reinhardtii* as revealed by noninvasive techniques in vivo, Proc. Natl. Acad. Sci. U. S. A. 111 (13) (2014) 5042–5047.
[97] C. Ünlü, B. Drop, R. Croce, H. van Amerongen, State transitions in *Chlamydomonas reinhardtii* strongly modulate the functional size of photosystem II but not of photosystem I, Proc. Natl. Acad. Sci. U. S. A. 111 (9) (2014) 3460–3465.
[98] J. Rochaix, Regulation and dynamics of the light-harvesting system, Annu. Rev. Plant Biol. 65 (2014) 287–309.
[99] H. Takahashi, S. Clowez, F. Wollman, O. Vallon, F. Rappaport, Cyclic electron flow is redox-controlled but independent of state transition, Nat. Commun. 4 (2013).
[100] P. Muller, X. Li, K. Niyogi, Non-photochemical quenching. A response to excess light energy, Plant Physiol. 125 (4) (2001) 1558–1566.
[101] Govindjee, M. Seufferheld, Non-photochemical quenching of chlorophyll a fluorescence: early history and characterization of two xanthophyll-cycle mutants of *Chlamydomonas reinhardtii*, Funct. Plant Biol. 29 (10) (2002) 1141–1155.
[102] O. Holub, M. Seufferheld, C. Govindjee, G. Heiss, R. Clegg, Fluorescence lifetime imaging microscopy of *Chlamydomonas reinhardtii*: non-photochemical quenching mutants and the effect of photosynthetic inhibitors on the slow chlorophyll fluorescence transient, J. Microsc. 226 (2) (2007) 90–120.
[103] M. Nilkens, E. Kress, P. Lambrev, Y. Miloslavina, M. Müller, A.R. Holzwarth, P. Jahns, Identification of a slowly inducible zeaxanthin-dependent component of non-photochemical quenching of chlorophyll fluorescence generated under steady-state conditions in Arabidopsis, Biochim. Biophys. Acta 1797 (4) (2010) 466–475.
[104] P. Jahns, A.R. Holzwarth, The role of the xanthophyll cycle and of lutein in photoprotection of photosystem II, Biochim. Biophys. Acta 1817 (1) (2012) 182–193.
[105] A.V. Ruban, M.P. Johnson, C.D. Duffy, The photoprotective molecular switch in the photosystem II antenna, Biochim. Biophys. Acta Bioenerg. 1817 (1) (2012) 167–181.
[106] E. Tyystjärvi, Photoinhibition of photosystem II, Int. Rev. Cell Mol. Biol. 300 (2013) 243–303.
[107] M. Iwai, M. Yokono, N. Inada, J. Minagawa, Live-cell imaging of photosystem II antenna dissociation during state transitions, Proc. Natl. Acad. Sci. U. S. A. 107 (5) (2010) 2337–2342.
[108] G.C. Papageorgiou, Govindjee, The non-photochemical quenching of the electronically excited state of chlorophyll a in plants: definitions, timelines, viewpoints, open questions, in: B. Demmig-Adams, G. Garab, W.W.I. Adams, Govindjee (Eds.), Non-photochemical Quenching and Energy Dissipation in Plants, Algae and Cyanobacteria, Advances in Photosynthesis and Respiration, vol. 40, Springer, Dordrecht 2014, pp. 1–44.
[109] G. Bonente, F. Passarini, S. Cazzaniga, C. Mancone, M.C. Buia, M. Tripodi, R. Bassi, S. Caffarri, The occurrence of the psbS gene product in *Chlamydomonas reinhardtii* and in other photosynthetic organisms and its correlation with energy quenching, Photochem. Photobiol. 84 (6) (2008) 1359–1370.
[110] G. Bonente, M. Ballottari, T.B. Truong, T. Morosinotto, T.K. Ahn, G.R. Fleming, K.K. Niyogi, R. Bassi, Analysis of LhcSR3, a protein essential for feedback de-excitation in the green alga *Chlamydomonas reinhardtii*, PLoS Biol. 9 (1) (2011) e1000577.
[111] R. Tokutsu, J. Minagawa, Energy-dissipative supercomplex of photosystem II associated with LHCSR3 in *Chlamydomonas reinhardtii*, Proc. Natl. Acad. Sci. U. S. A. 110 (24) (2013) 10016–10021.
[112] G. Peers, T.B. Truong, E. Ostendorf, A. Busch, D. Elrad, A.R. Grossman, M. Hippler, K.K. Niyogi, An ancient light-harvesting protein is critical for the regulation of algal photosynthesis, Nature 462 (7272) (2009) 518–521.
[113] G. Finazzi, G.N. Johnson, L. Dall'Osto, F. Zito, G. Bonente, R. Bassi, F. Wollman, Nonphotochemical quenching of chlorophyll fluorescence in Chlamydomonas reinhardtii, Biochemistry 45 (5) (2006) 1490–1498.
[114] P. Cardol, J. Alric, J. Girard-Bascou, F. Franck, F.A. Wollman, G. Finazzi, Impaired respiration discloses the physiological significance of state transitions in Chlamydomonas, Proc. Natl. Acad. Sci. U. S. A. 106 (37) (2009) 15979–15984.
[115] K.N. Ferreira, T.M. Iverson, K. Maghlaoui, J. Barber, S. Iwata, Architecture of the photosynthetic oxygen-evolving center, Science 303 (5665) (2004) 1831–1838.
[116] J.W. Hong, S. Jo, H. Yoon, Research and development for algae-based technologies in Korea: a review of algae biofuel production, Photosynth. Res. 123 (3) (2015) 297–303.
[117] B.A. Rasala, S.P. Mayfield, Photosynthetic biomanufacturing in green algae; production of recombinant proteins for industrial, nutritional, and medical uses, Photosynth. Res. 123 (3) (2015) 227–239.
[118] M.T. Guarnieri, P.T. Pienkos, Algal omics: unlocking bioproduct diversity in algae cell factories, Photosynth. Res. 123 (3) (2015) 255–263.